Radiative decays of double heavy baryons in a relativistic constituent three-quark model including hyperfine mixing effects

Tanja Branz,[1] Amand Faessler,[1] Thomas Gutsche,[1] Mikhail A. Ivanov,[2] Jürgen G. Körner,[3] Valery E. Lyubovitskij,[1,*] and Bettina Oexl[1]

[1]*Institut für Theoretische Physik, Universität Tübingen, Kepler Center for Astro and Particle Physics, Auf der Morgenstelle 14, D-72076 Tübingen, Germany*

[2]*Bogoliubov Laboratory of Theoretical Physics, Joint Institute for Nuclear Research, 141980 Dubna, Russia*

[3]*Institut für Physik, Johannes Gutenberg-Universität, D-55099 Mainz, Germany*

(Received 12 May 2010; published 25 June 2010)

We study flavor-conserving radiative decays of double-heavy baryons using a manifestly Lorentz covariant constituent three-quark model. Decay rates are calculated and compared to each other in the full theory, keeping masses finite, and also in the heavy quark limit. We discuss in some detail hyperfine mixing effects.

DOI: 10.1103/PhysRevD.81.114036 PACS numbers: 12.39.Ki, 13.30.Ce, 14.20.Lq, 14.20.Mr

I. INTRODUCTION

A first observation of the double charmed baryon $\Xi_{cc}^{+}(3519)$ by the SELEX Collaboration at Fermilab [1] stimulated theoretical studies of double-heavy baryons (DHBs). Up to now the study of DHBs has mainly focused on their mass spectra and their semileptonic decays (for an overview see e.g. Refs. [2,3]). In particular, significant progress has been achieved in the analysis of the DHB semileptonic weak decays. The current-induced flavor-changing double-heavy baryon transitions have been analyzed in a number of model approaches. These include effective field theories based on heavy quark spin symmetry [4–7], three-quark models [8–11], quark-diquark models [12,13], and nonrelativistic QCD sum rules [2,14]. Recently [3] we have presented a comprehensive analysis of the semileptonic decays of DHBs using a manifestly Lorentz covariant field theory approach termed the relativistic constituent three-quark model (RTQM) [3,8,15]. We considered all possible current-induced spin transitions between double-heavy baryons containing both types of light quarks—nonstrange $q = u, d$ and strange s. These involved the flavor-changing transitions $bc \to cc$ and $bb \to bc$. Form factors and decay rates have been calculated and have been compared to each other in the full theory with all masses finite and also in the heavy quark limit (HQL). Such an analysis is important because the semileptonic decays of DHBs provide yet another opportunity to measure the Cabibbo-Kobayashi-Maskawa (CKM) matrix element V_{cb}. This is particularly true since the transition matrix elements between double-heavy baryons obey spin symmetry relations in the heavy quark limit in addition to a model-independent zero recoil normalization of the relevant transition matrix elements.

In this paper we continue the study of DHB properties in the RTQM [3,15]. In particular, we analyze flavor-conserving radiative transitions between ground state DHBs: $1/2^+ \to 1/2^+$ and $3/2^+ \to 1/2^+$. The first estimate of the radiative decay widths of the DHBs in the heavy quark limit including hyperfine mixing effects has been done in Ref. [11] (for radiative transitions between DHBs see also the early paper [16]). A detailed analysis of DHB decays containing only the (bc) heavy quark configuration has been considered recently in Ref. [17]. As in our recent paper [3], we take the DHBs to be bound states of a light quark and a double-heavy $(Q_1 Q_2)$ diquark.

The origin of the hyperfine mixing for double-heavy baryons is the one-gluon exchange interaction between the light and heavy quarks in the DHB states containing two different heavy quarks—b and c. It leads to mixing of the states containing spin-0 and spin-1 heavy quark configurations. As shown in Refs. [10,11,17] hyperfine mixing has a big impact on the decay properties of double-heavy baryons. Both the weak semileptonic and the electromagnetic decay rates involving mixed DHB states are significantly enhanced or reduced relative to the rates involving unmixed states.

The RTQM can be viewed as an effective quantum field theory approach based on an interaction Lagrangian of hadrons interacting with their constituent quarks. From such an approach one can derive universal and reliable predictions for exclusive processes involving both mesons composed of a quark and antiquark and baryons composed of three quarks. The coupling strength of a hadron H to its constituent quarks is determined by the compositeness condition $Z_H = 0$ [18,19], where Z_H is the wave function renormalization constant of the hadron H. The quantity $Z_H^{1/2}$ is the matrix element between the physical particle state and the corresponding bare state. The compositeness condition $Z_H = 0$ enables one to represent a bound state by introducing a hadronic field interacting with its constituents so that the renormalization factor is equal to zero. This does not mean that we can solve the QCD bound state equations but we are able to show that the condition

*On leave from Department of Physics, Tomsk State University, 634050 Tomsk, Russia.

$Z_H = 0$ provides an effective and self-consistent way to describe the coupling of a hadron to its constituents. One starts with an effective interaction Lagrangian written down in terms of quark and hadron variables. Then, by using Feynman rules, the S-matrix elements describing hadron-hadron interactions are given in terms of a set of quark level Feynman diagrams. In particular, the compositeness condition enables one to avoid the problem of double counting of quark and hadronic degrees of freedom. The approach is self-consistent and all calculations of physical observables are straightforward. There is a small set of model parameters: the values of the constituent quark masses and the scale parameters that define the size of the distribution of the constituent quarks inside a given hadron.

The main objective of the present paper is to present an analysis of all possible electromagnetic transitions between ground state DHBs containing both types of light quarks—nonstrange $q = u, d$ and strange s. The paper is structured as follows. First, in Sec. II we review our relativistic constituent three-quark model approach (for more details see e.g. [3]) including a discussion on how to obtain a gauge-invariant coupling of the photon in our model. In Sec. III we discuss in more detail various aspects of the radiative decays of DHBs. We discuss the calculation of the relevant radiative transition matrix elements and analyze the consequences of taking the heavy quark limit for the radiative transitions. In Sec. IV we discuss in some detail hyperfine mixing effects in the radiative decays of DHBs. Section V contains our numerical results, which are compared to the predictions of a naive nonrelativistic quark model that has the same spin-flavor symmetry group as our DHB currents in the nonrelativistic limit. We also compare the results of the full finite mass calculation with results derived in the HQL. In addition we compare our results for $bc \to bc$ radiative transitions with recent quark model results [17]. Finally, in Sec. VI we present a brief summary of our results.

II. FRAMEWORK

A. Lagrangian

For the evaluation of the radiative decays of DHBs we will consistently employ the RTQM [3,15]. The model is based on an interaction Lagrangian describing the coupling between a baryon $B(q_1q_2q_3)$ and its constituent quarks q_1, q_2, and q_3. For $J^P = \frac{1}{2}+$ and $\frac{3}{2}+$ baryons the Lagrangians read

$$\begin{aligned}\mathcal{L}^{\rm str}_{\rm int}(x) = {} & g_B \bar{B}(x) \int dx_1 \int dx_2 \int dx_3 F(x, x_1, x_2, x_3) \\ & \times J_B(x_1, x_2, x_3) \\ & + g_{B^*} \bar{B}^*_\mu(x) \int dx_1 \int dx_2 \int dx_3 F(x, x_1, x_2, x_3) \\ & \times J^\mu_{B^*}(x_1, x_2, x_3) + \text{H.c.}, \end{aligned} \tag{1}$$

where J_B and J_{B^*} are interpolating three-quark currents with the quantum numbers of the relevant baryon $B(\frac{1}{2}^+)$ and $B^*(\frac{3}{2}^+)$. Note that the spin 3/2 spinor corresponding to the $B^*(\frac{3}{2}^+)$ field satisfies subsidiary Rarita-Schwinger conditions (see further details in Appendix A).

One has

$$J_B(x_1, x_2, x_3) = \varepsilon^{a_1a_2a_3} \Gamma_1 q^{a_3}(x_3) Q_1^{a_1}(x_1) C\Gamma_2 Q_2^{a_2}(x_2), \tag{2}$$

$$J^\mu_{B^*}(x_1, x_2, x_3) = \varepsilon^{a_1a_2a_3} \Gamma_1 q^{a_3}(x_3) Q_1^{a_1}(x_1) C\Gamma_2^\mu Q_2^{a_2}(x_2), \tag{3}$$

where the $\Gamma_{1,2}$ are strings of Dirac matrices, C is the charge conjugation matrix $C = \gamma^0\gamma^2$, and the a_i $(i = 1, 2, 3)$ are color indices. $F(x, x_1, x_2, x_3)$ is a nonlocal scalar vertex function which characterizes the finite size of the baryons.

The full Lagrangian

$$\mathcal{L}_{\rm full}(x) = \mathcal{L}_{\rm free}(x) + \mathcal{L}^{\rm em(1)}_{\rm int}(x) + \mathcal{L}^{\rm str+em(2)}_{\rm int}(x) \tag{4}$$

needed for the calculation of the radiative decays of DHBs includes the free parts of the baryons and the constituent quarks

$$\begin{aligned}\mathcal{L}_{\rm free}(x) = {} & \bar{B}(x)\mathcal{D}_B B(x) - \bar{B}^*_\mu(x)\mathcal{D}^{\mu\nu}_{B^*} B^*_\nu \\ & + \sum_{\psi=q,Q} \bar{\psi}(x)\mathcal{D}_\psi \psi(x), \end{aligned} \tag{5}$$

where

$$\begin{aligned}\mathcal{D}_\psi &= i\partial\!\!\!/ - m_\psi, \\ \mathcal{D}_B &= i\partial\!\!\!/ - m_B, \\ \mathcal{D}^{\mu\nu}_{B^*} &= g^{\mu\nu}(i\partial\!\!\!/ - m_{B^*}) - i(\gamma^\mu\partial^\nu + \gamma^\nu\partial^\mu) + \gamma^\mu i\partial\!\!\!/\gamma^\nu \\ &\quad - m_{B^*}\gamma^\mu\gamma^\nu. \end{aligned} \tag{6}$$

The baryon and constituent quark masses are denoted by $m_{B(B^*)}$ and m_ψ, respectively.

The electromagnetic interaction Lagrangian contains two pieces given by

$$\mathcal{L}^{\rm em}_{\rm int} = \mathcal{L}^{\rm em(1)}_{\rm int} + \mathcal{L}^{\rm em(2)}_{\rm int}, \tag{7}$$

which are generated after the inclusion of photons. The first term $\mathcal{L}^{\rm em(1)}_{\rm int}$ is generated via minimal substitution in the free Lagrangian $\mathcal{L}_{\rm free}$:

$$\partial^\mu\Psi \to (\partial^\mu - ie_\Psi A^\mu)\Psi, \qquad \partial^\mu\bar{\Psi} \to (\partial^\mu + ie_\Psi A^\mu)\bar{\Psi}, \tag{8}$$

where Ψ stands for B, B^*, q, and Q and e_Ψ is the electric charge of the field Ψ. The interaction Lagrangian $\mathcal{L}^{\rm em(1)}_{\rm int}$ reads

$$\mathcal{L}_{\rm int}^{\rm em(1)}(x) = e_B \bar{B}(x) \not{A} B(x) - e_{B^*} \bar{B}^*_\mu(x) (\not{A} g^{\mu\nu} + \gamma^\mu \not{A} \gamma^\nu - \gamma^\mu A^\nu - \gamma^\nu A^\mu) B^*_\nu(x) + \sum_{\psi=q,Q} e_\psi \bar{\psi}(x) \not{A} \psi(x). \quad (9)$$

The second electromagnetic interaction term $\mathcal{L}_{\rm int}^{\rm em(2)}$ is generated when one gauges the nonlocal Lagrangian Eq. (1). The gauging proceeds in a way suggested and extensively used in Refs. [15,20,21]. In order to guarantee local electromagnetic gauge invariance of the strong interaction Lagrangian one multiplies each quark field in $\mathcal{L}_{\rm int}^{\rm str}$ with a gauge field exponential. One then has

$$\mathcal{L}_{\rm int}^{\rm str+em(2)}(x) = g_B \bar{B}(x) \int dx_1 \int dx_2 \int dx_3 F(x, x_1, x_2, x_3) \epsilon^{a_1 a_2 a_3} \Gamma_1 e^{-ie_q I(x_3,x,P)} q^{a_3}(x_3) e^{-ie_{Q_1} I(x_1,x,P)} Q_1^{a_1}(x_1) \times C\Gamma_2 e^{-ie_{Q_2} I(x_2,x,P)} Q_2^{a_2}(x_2), + g_{B^*} \bar{B}^*_\mu(x) \int dx_1 \int dx_2 \int dx_3 F(x, x_1, x_2, x_3) \epsilon^{a_1 a_2 a_3} \Gamma_1 e^{-ie_q I(x_3,x,P)} q^{a_3}(x_3) \times e^{-ie_{Q_1} I(x_1,x,P)} Q_1^{a_1}(x_1) C\Gamma_2^\mu e^{-ie_{Q_2} I(x_2,x,P)} Q_2^{a_2}(x_2) + \text{H.c.}, \quad (10)$$

where

$$I(x_i, x, P) = \int_x^{x_i} dz_\mu A^\mu(z). \quad (11)$$

An expansion of the gauge exponential up to a certain power of A^μ leads to the terms contained in $\mathcal{L}_{\rm int}^{\rm em(2)}$.

The full Lagrangian consistently generates all the required matrix elements of the radiative decays of the DHBs. The relevant transitions can be represented by a set of quark loop diagrams. In the evaluation of the quark loops we use the free fermion propagator for the constituent quarks as dictated by the free quark Lagrangian discussed above. One has

$$iS_\psi(x-y) = \langle 0|T\psi(x)\bar{\psi}(y)|0\rangle = \int \frac{d^4k}{(2\pi)^4 i} e^{-ik(x-y)} \tilde{S}_\psi(k), \quad (12)$$

where

$$\tilde{S}_\psi(k) = \frac{1}{m_\psi - \not{k} - i\epsilon} \quad (13)$$

is the usual free fermion propagator in momentum space. We avoid the appearance of unphysical imaginary parts in Feynman diagrams by postulating that the baryon mass is less than the sum of the constituent quark masses $m_{B(B^*)} < m_q + m_{Q_1} + m_{Q_2}$, which is satisfied in our calculation. We mention that we have recently introduced a further refinement of our model in that we can now include quark confinement effects [22].

The free propagators of the baryon fields in momentum space are given by

$$\tilde{S}_B(k) = \frac{1}{m_B - \not{k} - i\epsilon}, \quad (14)$$

$$\tilde{S}^{\mu\nu}_{B^*}(k) = \frac{1}{m_{B^*} - \not{k} - i\epsilon}\left(-g^{\mu\nu} + \frac{1}{3}\gamma^\mu\gamma^\nu + \frac{2k^\mu k^\nu}{3m_{B^*}^2} + \frac{k^\nu\gamma^\mu - k^\mu\gamma^\nu}{3m_{B^*}}\right). \quad (15)$$

Next we consider in detail the required building blocks of the strong interaction Lagrangian $\mathcal{L}_{\rm int}^{\rm str}$—the vertex function F, the interpolating three-quark currents J_B and $J^\mu_{B^*}$, and the baryon-quark coupling constants g_B and g_{B^*}.

B. Vertex function

The vertex function F_B is related to the scalar part of the Bethe-Salpeter amplitude and characterizes the finite size of the baryon. In our approach we use a specific form for the vertex function given by

$$F(x, x_1, x_2, x_3) = N\delta^{(4)}\left(x - \sum_{i=1}^3 w_i x_i\right)\Phi\left(\sum_{i<j}(x_i - x_j)^2\right), \quad (16)$$

which is Poincaré-invariant. Φ is a nonlocal correlation function involving the three constituent quarks with masses m_1, m_2, and m_3; $N = 9$ is a normalization factor. The variable w_i is defined by $w_i = m_i/(m_1 + m_2 + m_3)$.

The Fourier transform of the correlation function $\Phi(\sum_{i<j}(x_i - x_j)^2)$ can be calculated by using Jacobi coordinates. One has

$$\Phi(p_1, p_2, p_3) = N\int dx e^{-ipx} \prod_{i=1}^3 \int dx_i e^{ip_i x_i} \times \delta^{(4)}\left(x - \sum_{i=1}^3 w_i x_i\right)\Phi\left(\sum_{i<j}(x_i - x_j)^2\right) = (2\pi)^4 \delta^{(4)}\left(p - \sum_{i=1}^3 p_i\right)\Phi(-l_1^2 - l_2^2), \quad (17)$$

where the Jacobi coordinates are defined by

$$
\begin{aligned}
x_1 &= x + \frac{1}{\sqrt{2}}\xi_1 w_3 - \frac{1}{\sqrt{6}}\xi_2(2w_2 + w_3),\\
x_2 &= x + \frac{1}{\sqrt{2}}\xi_1 w_3 + \frac{1}{\sqrt{6}}\xi_2(2w_1 + w_3),\\
x_3 &= x - \frac{1}{\sqrt{2}}\xi_1(w_1 + w_2) + \frac{1}{\sqrt{6}}\xi_2(w_1 - w_2).
\end{aligned}
\tag{18}
$$

The corresponding Jacobi momenta read

$$
\begin{aligned}
p &= p_1 + p_2 + p_3,\\
l_1 &= \frac{1}{\sqrt{2}} w_3(p_1 + p_2) - \frac{1}{\sqrt{2}}(w_1 + w_2)p_3,\\
l_2 &= -\frac{1}{\sqrt{6}}(2w_2 + w_3)p_1 + \frac{1}{\sqrt{6}}(2w_1 + w_3)p_2\\
&\quad + \frac{1}{\sqrt{6}}(w_1 - w_2)p_3,
\end{aligned}
\tag{19}
$$

where, according to Eq. (16), $\sum_{i=1}^{3} w_i x_i = x$. Since the function $\Phi(\sum_{i<j}(x_i - x_j)^2)$ is invariant under translations its Fourier transform only depends on two four-momenta. The function $\Phi(-l_1^2 - l_2^2)$ in Eq. (17) will be modeled by a Gaussian form in our approach. The minus sign in the argument is chosen to emphasize that we are working in Minkowski space. Our choice is the Gaussian form

$$
\Phi(-l_1^2 - l_2^2) = \exp(18(l_1^2 + l_2^2)/\Lambda^2), \tag{20}
$$

where the parameter Λ characterizes the size of the DHB. Since l_1^2 and l_2^2 turn into $-l_1^2$ and $-l_2^2$ in Euclidean space the form (20) has the appropriate falloff behavior in the Euclidean region.

C. Three-quark currents

In the so-called Q_1Q_2 basis the DHBs are classified by the set of quantum numbers (J^P, S_d), where J^P is the spin parity of the baryon state and S_d is the spin of the heavy diquark. There are two types of heavy diquarks—those with $S_d = 0$ (antisymmetric spin configuration $[Q_1Q_2]$) and those with $S_d = 1$ (symmetric spin configuration $\{Q_1Q_2\}$). Accordingly there are two $J^P = 1/2^+$ DHB states. We follow the standard convention and attach a prime to the $S_d = 0$ states whereas the $S_d = 1$ states are unprimed. The $J^P = 3/2^+$ states are in the symmetric heavy quark spin configuration. In Table I we list the quantum numbers of the double-heavy baryons including their mass spectrum as calculated in [13].

As we have discussed in our recent paper [3], there is a mass inversion in the $(1/2^+)$ mixed flavor states (Ξ_{bc}, Ξ'_{bc}) and $(\Omega_{bc}, \Omega'_{bc})$ in that $M(\Xi'_{bc}) > M(\Xi_{bc})$ and $M(\Omega'_{bc}) > M(\Omega_{bc})$ even though the heavy diquarks satisfy the conventional hyperfine splitting pattern $m_{(bc)_{S=1}} > m_{(bc)_{S=0}}$. This inversion is a feature of all models that have attempted to calculate the mass spectrum of double-heavy baryons [2,9,13,24–26]. In particular, the inverted mass hierarchy implies that one can only expect substantial flavor-changing branching ratios for the two lowest-lying states Ξ_{bc} and Ω_{bc} whereas the rates of the higher lying states Ξ'_{bc}, Ξ^*_{bc} and Ω'_{bc}, Ω^*_{bc} will be dominated by flavor-preserving one-photon transitions to the lowest-lying states Ξ_{bc} and Ω_{bc}. One of the purposes of the present paper is to analyze the strength of the one-photon transitions between the $S_d = 0$ and $S_d = 1$ double-heavy baryon states. In the HQL, the photon couples to the light quark only, and therefore one-photon transitions between the $S_d = 0$ and $S_d = 1$ double-heavy baryon states such as $\Xi'_{bc} \to \Xi_{bc} + \gamma$ are forbidden in this limit. For finite heavy quark masses one-photon transitions between the $S_d = 0$ and $S_d = 1$ double-heavy baryon states will occur at a somewhat reduced rate which, however, is very likely to exceed the flavor-changing weak decay rates of these states [16].

TABLE I. Classification and mass values of double-heavy baryons. Mass values are based on [13] except for the Ξ_{cc} mass which is taken from [23].

Notation	Content	J^P	S_d	Mass (GeV)
Ξ_{cc}	$q\{cc\}$	$1/2^+$	1	3.5189
Ξ_{bc}	$q\{bc\}$	$1/2^+$	1	6.933
Ξ'_{bc}	$q[bc]$	$1/2^+$	0	6.963
Ξ_{bb}	$q\{bb\}$	$1/2^+$	1	10.202
Ξ^*_{cc}	$q\{cc\}$	$3/2^+$	1	3.727
Ξ^*_{bc}	$q\{bc\}$	$3/2^+$	1	6.980
Ξ^*_{bb}	$q\{bb\}$	$3/2^+$	1	10.237
Ω_{cc}	$s\{cc\}$	$1/2^+$	1	3.778
Ω_{bc}	$s\{bc\}$	$1/2^+$	1	7.088
Ω'_{bc}	$s[bc]$	$1/2^+$	0	7.116
Ω_{bb}	$s\{bb\}$	$1/2^+$	1	10.359
Ω^*_{cc}	$s\{cc\}$	$3/2^+$	1	3.872
Ω^*_{bc}	$s\{bc\}$	$3/2^+$	1	7.130
Ω^*_{bb}	$s\{bb\}$	$3/2^+$	1	10.389

Following the suggestion of Ref. [10] (see also discussion in [11]) we also consider hyperfine $\Xi'_{bc} - \Xi_{bc}$ and $\Omega'_{bc} - \Omega_{bc}$ mixing induced by one-gluon exchange interactions. We define the mixed states through the unmixed states using a unitary transformation [10,11] with the mixing angles θ_Ξ or θ_Ω:

$$
\begin{pmatrix} B^h_{bc} \\ B^l_{bc} \end{pmatrix} = \begin{pmatrix} \cos\theta_B & \sin\theta_B \\ -\sin\theta_B & \cos\theta_B \end{pmatrix} \begin{pmatrix} B'_{bc} \\ B_{bc} \end{pmatrix}, \tag{21}
$$

where $B = \Xi$ or Ω. We treat the mixing angle θ_B as a quantity of order $\mathcal{O}(\alpha_s)$, where α_s is the QCD coupling constant. By B^h and B^l we denote the mixed states with the mass hierarchy $m_{B_l} < m_B < m_{B'} < m_{B_h}$. The masses of the mixed states m_{B_h} and m_{B_l} differ from the masses of the unmixed states by small hyperfine splitting corrections. They are expressed through the unmixed masses and mixing angle as

$$m_{B_h} = m_{B'} + (m_{B'} - m_B)\frac{\sin^2\theta}{\cos 2\theta},$$
$$m_{B_l} = m_B - (m_{B'} - m_B)\frac{\sin^2\theta}{\cos 2\theta}. \quad (22)$$

When diagonalizing the mass matrix of the unmixed states the diagonal elements are driven apart such that the mass difference of the mixed states is larger than that of the unmixed states. One has

$$m_{B_h} - m_{B_l} = \frac{m_{B'} - m_B}{\cos 2\theta}. \quad (23)$$

This leads to a further enhancement of the widths of the radiative transitions $B^h_{bc} \to B^l_{bc} + \gamma$ between mixed states, because the photon transition rate is proportional to $(M_1 - M_2)^3$ (see Appendix A).

The mixing angle θ_B corresponds to the combination $\theta + 30°$ in [11]: $\theta_B \equiv \theta + 30°$. Here θ is the angle that rotates the mixed B^h, B^l states into the $\hat{B}$, $\hat{B}'$ states—bound states of the b quark and the heavy-light cq diquark (so-called qc basis). The angle 30° corresponds to a further rotation of the $\hat{B}$, $\hat{B}'$ states into the unmixed B', B states defined in the bc basis (i.e. bound states of the light quark and heavy bc diquark). In the quark model calculation of [11] one obtains $\sin\theta_\Xi = 0.431$ ($\theta_\Xi = 25.5°$) and $\sin\theta_\Omega = 0.437$ ($\theta_\Omega = 25.9°$). Using these values of the mixing angle θ and the masses of unmixed states we deduce the following values for the masses of the mixed states:

$$m_{\Xi^h_{bc}} = 6.972 \text{ MeV}, \qquad m_{\Xi^l_{bc}} = 6.924 \text{ MeV},$$
$$m_{\Omega^h_{bc}} = 7.125 \text{ MeV}, \qquad m_{\Omega^l_{bc}} = 7.079 \text{ MeV}. \quad (24)$$

The interpolating currents of the DHB states $B_{qQ_1Q_2}$ are constructed in the form of a light quark q^{a_3} coupled to a heavy diquark $D^{a_3}_{Q_1Q_2}$. One obtains

$$J_{qQ_1Q_2} = \Gamma^q_{Q_1Q_2} q^{a_3}_3 D^{a_3}_{Q_1Q_2},$$
$$D^{a_1}_{Q_1Q_2} = \varepsilon^{a_1a_2a_3}(Q^{a_1}_1 C\Gamma^D_{Q_1Q_2} Q^{a_2}_2). \quad (25)$$

For the $(\frac{1}{2}^+, 0)$, $(\frac{1}{2}^+, 1)$, and $(\frac{3}{2}^+, 1)$ states we use the simplest currents—the pseudoscalar J^P, the vector J^V, and J^V_μ currents, respectively:

$$J^P_{qQ_1Q_2} = \varepsilon^{a_1a_2a_3} q^{a_3}(Q^{a_1}_1 C\gamma_5 Q^{a_2}_2), \quad (26a)$$
$$J^V_{qQ_1Q_2} = \varepsilon^{a_1a_2a_3}\gamma^\alpha\gamma^5 q^{a_3}(Q^{a_1}_1 C\gamma_\alpha Q^{a_2}_2), \quad (26b)$$
$$J^V_{qQ_1Q_2,\mu} = \varepsilon^{a_1a_2a_3} q^{a_3}(Q^{a_1}_1 C\gamma_\mu Q^{a_2}_2). \quad (26c)$$

In the heavy quark limit the above currents reduce to

$$j^P_{qQ_1Q_2} = \varepsilon^{a_1a_2a_3}\psi^{a_3}_q(\psi^{a_1}_{Q_1}\sigma_2\psi^{a_2}_{Q_2}), \quad (27a)$$
$$j^V_{qQ_1Q_2} = \varepsilon^{a_1a_2a_3}\vec{\sigma}\psi^{a_3}_q(\psi^{a_1}_{Q_1}\sigma_2\vec{\sigma}\psi^{a_2}_{Q_2}), \quad (27b)$$
$$\vec{j}^V_{qQ_1Q_2} = \varepsilon^{a_1a_2a_3}\psi^{a_3}_q(\psi^{a_1}_{Q_1}\sigma_2\vec{\sigma}\psi^{a_2}_{Q_2}), \quad (27c)$$

TABLE II. DHB wave functions.

Baryon	Wave function	Baryon	Wave function
Ξ_{cc}	$qcc\ \chi_S(\lambda)$	Ω_{cc}	$scc\ \chi_S(\lambda)$
Ξ_{bb}	$qbb\ \chi_S(\lambda)$	Ω_{bb}	$sbb\ \chi_S(\lambda)$
Ξ_{bc}	$\frac{1}{\sqrt{2}}q(bc+cb)\ \chi_S(\lambda)$	Ω_{bc}	$\frac{1}{\sqrt{2}}s(bc+cb)\ \chi_S(\lambda)$
Ξ'_{bc}	$\frac{1}{\sqrt{2}}q(bc-cb)\ \chi_A(\lambda)$	Ω'_{bc}	$\frac{1}{\sqrt{2}}s(bc-cb)\ \chi_A(\lambda)$
Ξ^*_{cc}	$-qcc\ \chi^*_S(\lambda)$	Ω^*_{cc}	$-scc\ \chi^*_S(\lambda)$
Ξ^*_{bb}	$-qbb\ \chi^*_S(\lambda)$	Ω^*_{bb}	$-sbb\ \chi^*_S(\lambda)$
Ξ^*_{bc}	$-\frac{1}{\sqrt{2}}q(bc+cb)\ \chi^*_S(\lambda)$	Ω^*_{bc}	$-\frac{1}{\sqrt{2}}s(bc+cb)\ \chi^*_S(\lambda)$

where ψ_{q,Q_1,Q_2} are the upper components of the Dirac quark spinors and the σ_i are the Pauli spin matrices. Note that the spin-flavor wave function coincides with the nonrelativistic limit in the HQL. In the nonrelativistic limit our DHB currents have a one-to-one correspondence to the naive quark model baryon spin-flavor functions (up to overall factors) which are displayed in Table II. Further details on the naive quark model and how to evaluate the radiative transition amplitudes in this framework can be found in Appendix B.

According to the definition (21) the interpolating currents of the mixed B^h and B^l states are given by

$$\begin{pmatrix} g_{B^h} J^{B^h}_{qbc} \\ g_{B'} J^{B^l}_{qbc} \end{pmatrix} = \begin{pmatrix} \cos\theta_B & \sin\theta_B \\ -\sin\theta_B & \cos\theta_B \end{pmatrix} \begin{pmatrix} g_{B'} J^P_{qbc} \\ g_B J^V_{qbc} \end{pmatrix}. \quad (28)$$

D. Baryon-quark coupling constant

The coupling constants g_ψ ($\psi = B, B^*$) are determined by the compositeness condition [3,15,18,19]. The compositeness condition implies that the renormalization constant of the hadron wave function is set equal to zero, i.e.

$$Z_\psi = 1 - g^2_B \Sigma'_\psi(m_\psi) = 0. \quad (29)$$

$\Sigma'_\psi(m_\psi)$ is the derivative of the baryon mass operator shown in Fig. 1.

In the case of the $3/2^+$ states the function $\Sigma_{B^*}(p)$ is subtracted from the nonvanishing part of the mass operator $\Sigma^{\mu\nu}_{B^*}(p)$ proportional to the Minkowski metric tensor $g^{\mu\nu}$:

$$\bar{u}_\mu(p, s^*)\Sigma^{\mu\nu}_{B^*}(p)u_\nu(p, s^*) = \bar{u}_\mu(p, s^*)\Sigma_{B^*}(p)g^{\mu\nu}u_\nu(p, s^*), \quad (30)$$

where $u^\mu(p, s^*)$ is the $\frac{3}{2}$ spinor. Other possible Lorentz structure on the right-hand side of Eq. (30) vanish due to

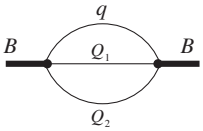

FIG. 1. Diagram describing the double-heavy baryon mass operator.

the Rarita-Schwinger conditions. Note that the compositeness condition is equivalent to a Ward identity relating the electromagnetic vertex function at zero momentum transfer to the derivative of the mass operator (see details e.g. in [3]). Explicit expressions for the baryon mass operators are given in Appendix C.

III. RADIATIVE DECAYS OF DOUBLE-HEAVY BARYONS

A. Matrix elements

In our approach the radiative decays of DHBs are described by the set of Feynman diagrams shown in Fig. 2. The three ''triangle'' diagrams [Fig. 2(a)–2(c)] are generated by the coupling of the constituent quarks with the photon. The two ''bubble'' diagrams in Fig. 2(d) and 2(e) are generated by gauging the nonlocal strong Lagrangian (see discussion in Sec. II). Finally the two ''pole'' diagrams in Fig. 2(f) and 2(g) are generated by the direct coupling of the initial/final baryon with the photon. Because of our explicit construction the DHB radiative matrix elements are explicitly gauge-invariant. The pole diagrams vanish for the radiative transitions $(\frac{1}{2}^+, 0) \to (\frac{1}{2}^+, 1)$ and $(\frac{3}{2}^+, 1) \to (\frac{1}{2}^+, 0)$ due to the orthogonality of the heavy diquark spin wave functions. For the same reason the photon does not couple to the light quarks in these modes implying that the corresponding triangle and bubble graphs vanish. For the $(\frac{3}{2}^+, 1) \to (\frac{1}{2}^+, 1)$ transitions the pole diagram in Fig. 2(g) vanishes due to the Rarita-Schwinger conditions for the $\frac{3}{2}$ spinor. All these statements are true for photon transitions between unmixed states. Photon transitions between mixed DHB states will be discussed in Sec. IV.

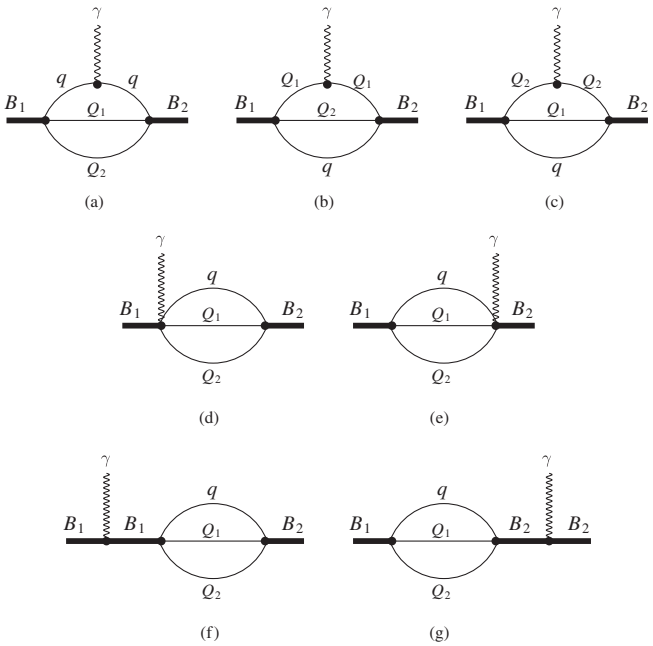

FIG. 2. Diagrams contributing to the radiative transitions of double-heavy baryons.

We continue with a summary of some useful analytical results. The on-shell matrix elements for the radiative transitions $\frac{1}{2} \to \frac{1}{2}$ and $\frac{3}{2} \to \frac{1}{2}$ are given by

$$M_\mu(1/2 \to 1/2) = \bar{u}_{B_2}(p_2, s_2)\Lambda_\mu(p_1, p_2)u_{B_1}(p_1, s_1),$$
$$M_\mu(3/2 \to 1/2) = \bar{u}_{B_2}(p_2, s_2)\Lambda_{\mu\nu}(p_1, p_2)u^\nu_{B^*_1}(p_1, s^*), \tag{31}$$

where $u_B(p, s)$ and $u^\nu_{B^*}(p, s^*)$ are the spin $\frac{1}{2}$ and $\frac{3}{2}$ spinors with the normalization (see further details in Appendix A):

$$\bar{u}_B(p, s)u_B(p, s) = 2m_B,$$
$$\bar{u}^\mu_{B^*}(p, s^*)u_{B^*_\mu}(p, s^*) = -2m_{B^*}. \tag{32}$$

The momenta of the final state photon and the initial and final state baryon are denoted by q, p_1, and p_2, respectively, where $q = p_1 - p_2$ and where s and s^* are spin indices. Because of gauge invariance the electromagnetic vertex function $\Lambda_\mu(p_1, p_2)$ is orthogonal to the photon momentum $q^\mu\Lambda_\mu(p_1, p_2) = 0$. As a result the vertex function $\Lambda_\mu(p_1, p_2)$ is given by the sum of the gauge-invariant pieces of the triangle (Δ), the bubble (bub), and the pole (pol) diagrams, while the nongauge-invariant parts of these diagrams cancel in the sum:

$$\Lambda_\mu(p_1, p_2) = \Lambda^\perp_{\mu,\Delta}(p_1, p_2) + \Lambda^\perp_{\mu,\mathrm{bub}}(p_1, p_2) + \Lambda^\perp_{\mu,\mathrm{pol}}(p_1, p_2). \tag{33}$$

The contribution of each diagram can be split into gauge-invariant and gauge-variant pieces by introducing the decomposition

$$\gamma_\mu = \gamma^\perp_\mu + q_\mu \frac{\not{q}}{q^2}, \qquad p_i = p^\perp_i + q_\mu \frac{p_i q}{q^2},$$
$$g_{\mu\nu} = g^\perp_{\mu\nu} + \frac{q_\mu q_\nu}{q^2}, \tag{34}$$

such that $\gamma^\perp_\mu q^\mu = 0$, $p^\perp_i q^\mu = 0$, and $g^\perp_{\mu\nu}q^\mu = 0$, where p_i is p_1 or p_2. The vertex function $\Lambda^\perp_\mu(p_1, p_2)$ can then be expressed in terms of $\gamma^\perp_\mu$, $p^\perp_{i\mu}$, and $g^\perp_{\mu\nu}$. Note that all matrix elements are finite for real photons ($q^2 = 0$). Doing our calculations we start with $q^2 \neq 0$ and then take the limit $q^2 \to 0$. Explicit expressions of the electromagnetic vertex functions can be found in Appendix C.

B. Heavy quark limit

In the HQL the masses of the heavy quarks are taken to infinity ($m_Q \to \infty$). In this limit the spins of the double-heavy diquark and the light quark in the DHB states decouple leading to a much simplified transition structure. In particular, the transition amplitudes $(\frac{1}{2}^+, 0) \to (\frac{1}{2}^+, 1)$ and $(\frac{3}{2}^+, 1) \to (\frac{1}{2}^+, 0)$ vanish as $\mathcal{O}(1/m_Q)$ since the photon coupling to the heavy quarks involves a spin-flip factor proportional to the magnetic moment of the heavy quark given by $\mu_Q = e_Q/(2m_Q)$. This is in full agreement with

the nonrelativistic quark model (for more details see the discussion in Appendix B) where the corresponding amplitudes are found to be proportional to the difference of the magnetic moments of the heavy quarks $\mu_c - \mu_b$. The transition amplitude $(\frac{3}{2}^+, 1) \to (\frac{1}{2}^+, 1)$ survives in the HQL since the photon can now couple to the light quark. Again, this is consistent with the nonrelativistic quark model. The structure of the amplitude of the $(\frac{3}{2}^+, 1) \to (\frac{1}{2}^+, 1)$ transition significantly simplifies in the HQL. Only the triangle diagram in Fig. 2(a) contributes to the transition amplitude since Fig. 2(a) represents the direct coupling of the light quark with the photon. The contribution of Fig. 2(a) scales as $\mathcal{O}(1)$ in the inverse heavy quark mass expansion. The other diagrams are suppressed in the HQL. In particular, the triangle diagrams in Fig. 2(b) and 2(c) contribute only at $\mathcal{O}(1/m_Q)$ since they represent direct couplings of the heavy quarks with the photon. The same holds true for the bubble diagrams in Fig. 2(d) and 2(e) involving a nonlocal photon-light quark coupling.

Following ideas developed in our paper [3], we choose the momenta of the initial and final DHB as $p_1^\mu = (m_{Q_1} + m_{Q_2})v^\mu$ and $p_2^\mu = (m_{Q_1} + m_{Q_2})v'^\mu = (m_{Q_1} + m_{Q_2})v^\mu + r^\mu$, where r is a small residual momentum in the sense that $r^2 \sim \mathcal{O}(1)$ when $m_{Q_i} \to \infty$. With these assumptions the heavy quark propagators simplify in the HQL. One has

$$\tilde{S}_{Q_i}(k_i \pm p\eta_i) \to \frac{1 \pm \not{v}}{2} \frac{1}{\mp k_i v - i\epsilon}, \tag{35}$$

where $\eta_i = m_{Q_i}/(m_{Q_1} + m_{Q_2})$.

In the HQL and at $q^2 = 0$ the explicitly gauge-invariant transition amplitude $(\frac{3}{2}^+, 1) \to (\frac{1}{2}^+, 1)$ is given by

$$\Lambda^\perp_{\mu\nu} = \Gamma^\perp_{\mu\nu} I_\Delta, \qquad I_\Delta = 24 N_f e_q g_{B_1^*} g_{B_2} R_{12}(m_q, \Lambda), \tag{36}$$

where N_f denotes a statistical flavor factor which is equal to 1 or 2 for DHBs with two different or two identical heavy quarks. $\Gamma^\perp_{\mu\nu} = (\gamma_\mu q_\nu - g_{\mu\nu}\not{q})\gamma_5$ is the Lorentz structure orthogonal to the photon momentum: $q^\mu \Gamma^\perp_{\mu\nu} = 0$. Note that only the Lorentz structure $\Gamma^\perp_{\mu\nu}$ survives in the HQL. As shown in Appendix A other possible structures vanish. The function $R_{12}(m_q, \Lambda)$ reads

$$R_{AB}(m_q, \Lambda) = \int \frac{d^4k_1}{(2\pi)^4 i} \int \frac{d^4k_2}{(2\pi)^4 i} \Phi^2(z) \frac{m_q + (k_2 - k_1)v}{(-k_1 v - i\epsilon)^A (k_2 v - i\epsilon)(m_q^2 - (k_2 - k_1)^2 - i\epsilon)^B}, \tag{37}$$

where $z = -\frac{2}{3}(k_1^2 - k_1 k_2 + k_2^2)$ and where A and B denote integer powers. The coupling constants $g_{B_1^*}$ and g_{B_2} are given by

$$\frac{1}{g^2_{B_1^*}} = \frac{1}{3 g^2_{B_2}} = 12 N_f R_{21}(m_q, \Lambda). \tag{38}$$

Using the Laplace transform

$$\Phi^2(z) = \int_0^\infty ds \Phi^L(s) e^{-sz}, \tag{39}$$

the integration over the virtual momenta k_1 and k_2 in $R_{AB}(m_q, \Lambda)$ can be done. One obtains

$$\begin{aligned} R_{21}(m_q, \Lambda) &= \frac{\Lambda^4}{(16\pi^2)^2} \int_0^\infty d\alpha_1 d\alpha_2 d\alpha_3 \frac{\alpha_1}{D^2} \\ &\quad \times \left(\frac{m_q}{\Lambda} + \frac{\alpha_1 + \alpha_2}{4D}\right) \Phi^2(y), \\ R_{12}(m_q, \Lambda) &= \frac{\Lambda^3}{(16\pi^2)^2} \int_0^\infty d\alpha_1 d\alpha_2 d\alpha_3 \frac{\alpha_3}{D^2} \\ &\quad \times \left(\frac{m_q}{\Lambda} + \frac{\alpha_1 + \alpha_2}{4D}\right) \Phi^2(y), \end{aligned} \tag{40}$$

where

$$\begin{aligned} D &= \frac{3}{4} + \alpha_3, \\ \frac{y}{\Lambda^2} &= \frac{2}{3}\left(\frac{m_q^2}{\Lambda^2}\alpha_3 + \frac{(1 + \alpha_3)(\alpha_1 - \alpha_2)^2 + \alpha_1\alpha_2}{4D}\right). \end{aligned} \tag{41}$$

For the $(\frac{3}{2}^+, 1) \to (\frac{1}{2}^+, 1)$ transition the HQL helicity amplitudes read

$$\begin{aligned} H_{\pm(1/2)\mp 1} &= \bar{\epsilon}^{*\mu}(\mp 1)\bar{u}\left(v, \pm\frac{1}{2}\right)\Lambda^\perp_{\mu\nu} u^\nu\left(v, \pm\frac{3}{2}\right) \\ &= \pm M_+ M_- \sqrt{\frac{M_2}{M_1}} I_\Delta, \end{aligned} \tag{42}$$

$$\begin{aligned} H_{\pm(1/2)\pm 1} &= \bar{\epsilon}^{*\mu}(\pm 1)\bar{u}\left(v, \pm\frac{1}{2}\right)\Lambda^\perp_{\mu\nu} u^\nu\left(v, \mp\frac{1}{2}\right) \\ &= \mp\sqrt{\frac{1}{3}} M_+ M_- \sqrt{\frac{M_2}{M_1}} I_\Delta. \end{aligned} \tag{43}$$

The ratio of the HQL helicity amplitudes is given by $H_{\pm(1/2)\mp 1}/H_{\pm(1/2)\pm 1} = -\sqrt{3}$; i.e. one has a pure $M1$ magnetic dipole transition. This coincides with the predictions of the nonrelativistic quark model (NQM) (see Appendix B), where

$$H_{\pm(1/2)\mp 1} = -\sqrt{3} H_{\pm(1/2)\pm 1} = \pm \frac{2\mu_q}{\sqrt{3}} M_+ M_- \sqrt{\frac{M_2}{M_1}}. \tag{44}$$

The function I_Δ appearing in (42) and (43) is given by

$$I_\Delta = \frac{2\mu_q}{\sqrt{3}}\beta, \tag{45}$$

where

$$\beta = 2m_q \frac{R_{12}(m_q,\Lambda)}{R_{21}(m_q,\Lambda)}. \tag{46}$$

In the HQL the helicity amplitudes, the form factors F_1 and F_2, and the decay rate of the $(\frac{3}{2}^+,1)\to(\frac{1}{2}^+,1)$ transition read

$$\begin{aligned} H_{\pm(1/2)\mp1} &= -\sqrt{3}H_{\pm(1/2)\pm1} = \pm\frac{2\mu_q}{\sqrt{3}}\beta M_+ M_- \sqrt{\frac{M_2}{M_1}}, \\ F_1 &= \frac{2\mu_q}{\sqrt{3}}\beta M_+ \sqrt{\frac{M_2}{M_1}}, \\ F_2 &= -\frac{4\mu_q}{\sqrt{3}}\beta\frac{M_2}{M_+}\sqrt{M_1 M_2}, \\ \Gamma_{(3/2)\to(1/2)^S} &= \frac{4}{3}K\mu_q^2\beta^2, \end{aligned} \tag{47}$$

where

$$K = \alpha M_2 \frac{(M_1^2 - M_2^2)^3}{6M_1^4}. \tag{48}$$

$\alpha \simeq 1/137$ is the fine-structure coupling constant and M_1 and M_2 are the masses of the parent and daughter baryon, respectively. The state $\frac{1}{2}^S$ corresponds to the baryon with symmetric heavy quark spin configuration.

It is evident that our HQL rate results differ from the predictions of the NQM by the factor β^2 defined in (46). In the NQM one has $\beta \equiv 1$ while in our covariant approach $\beta \approx 0.5$. It is for this reason that our HQL predictions for the $(\frac{3}{2}^+,1)\to(\frac{1}{2}^+,1)+\gamma$ decay widths are down by a factor of 4 compared to the predictions of the NQM.

IV. HYPERFINE MIXING AND RADIATIVE DECAYS OF MIXED STATES

As mentioned in the introduction the origin of the hyperfine mixing in the double-heavy baryons is the one-gluon exchange interaction between the light and heavy quarks in the states containing two different heavy quarks—b and c. The one-gluon interaction leads to mixing of the states containing spin-0 and spin-1 heavy quark configurations. In this section we discuss in some detail the calculations of DHB radiative decays involving mixed states. We have three types of transitions: $B_{bc}^h \to B_{bc}^l$, $B_{bc}^* \to B_{bc}^l$, and $B_{bc}^* \to B_{bc}^h$. All three modes are quite interesting, because their study opens the opportunity to determine the mixing angle θ and to measure the masses of the mixed states. In particular, the first mode $B_{bc}^h \to B_{bc}^l$ is interesting since it is described by transitions between baryon components with the same spin configuration of the heavy quarks $(\frac{1}{2}^+,1)\to(\frac{1}{2}^+,1)$ and $(\frac{1}{2}^+,0)\to(\frac{1}{2}^+,0)$. Because now the photon can also couple to the light quark one will have a corresponding enhancement of the decay rates. The two other modes $B_{bc}^* \to B_{bc}^l$ and $B_{bc}^* \to B_{bc}^h$ involve mixing of the leading $(\frac{3}{2}^+,1)\to(\frac{1}{2}^+,1)$ and subleading $(\frac{3}{2}^+,1)\to(\frac{1}{2}^+,0)$ amplitudes and are therefore also important for an analysis of the mixing angle θ. The matrix elements for transitions involving mixed states are derived using the transition matrix elements of the unmixed states. In Appendix B we present the results of the NQM for transitions involving mixed states in terms of quark magnetic moments and the mixing angle θ. In our numerical calculations we differentiate between the mixing angles for the Ξ states and the Ω states using the predictions of the quark model [11]: $\theta_\Xi \simeq 25.5°$ and $\theta_\Omega \simeq 25.9°$.

The last issue which we would like to discuss in this section is the HQL structure of transitions involving mixed states. As we have discussed in the previous section the leading contribution for the $B_{bc}^* \to B_{bc}^l$ and $B_{bc}^* \to B_{bc}^h$ transitions comes from the $(\frac{3}{2}^+,1)\to(\frac{1}{2}^+,1)$ transition generated by the direct coupling of the photon with the light quark [see diagram in Fig. 2(a)]. The corresponding amplitudes are multiplied by the factor $\cos\theta$ for the $B_{bc}^* \to B_{bc}^l$ mode and by $-\sin\theta$ for the $B_{bc}^* \to B_{bc}^h$ mode. In the case of the $B_{bc}^h \to B_{bc}^l$ transition the leading contribution is again generated by the direct light quark-photon coupling [Fig. 2(a)]. In this case one has to sum the two transitions involving a light quark spin flip $(\frac{1}{2}^+,0)\to(\frac{1}{2}^+,0)$ and $(\frac{1}{2}^+,1)\to(\frac{1}{2}^+,1)$. The calculation of these leading matrix elements follows the treatment in the previous section. In particular, the leading contribution to the matrix element of the $B_{bc}^h \to B_{bc}^l$ transition is expressed though the same structure integral $R_{12}(m_q,\Lambda)$ as in the case of the $(\frac{3}{2}^+,1)\to(\frac{1}{2}^+,1)$ transition

$$\begin{aligned} \Lambda_\mu^\perp &= \not{q}\gamma_\mu^\perp J_\Delta, \\ J_\Delta &= 24N_f e_q \sin(2\theta_B)\frac{g_B^2 + g_{B'}^2}{2}R_{12}(m_q,\Lambda), \end{aligned} \tag{49}$$

where g_B and g_B' are the coupling constants of the unmixed states $(\frac{1}{2}^+,1)$ and $(\frac{1}{2}^+,0)$:

$$\frac{1}{g_{B'}^2} = \frac{1}{3g_B^2} = 12N_f R_{21}(m_q,\Lambda). \tag{50}$$

In the HQL the helicity amplitudes of the $B_{bc}^h \to B_{bc}^l$ transition are given by

$$\begin{aligned} H_{\pm(1/2)\pm1} &= \bar\epsilon^{*\mu}(\pm1)\bar u\Big(v,\pm\frac{1}{2}\Big)\Lambda_\mu^\perp u\Big(v,\mp\frac{1}{2}\Big) \\ &= M_+ M_- \sqrt{\frac{2M_2}{M_1}}J_\Delta. \end{aligned} \tag{51}$$

After some straightforward algebra one can express the helicity amplitudes $H_{\pm(1/2)\pm1}$ in terms of the parameter β derived in Eq. (46). One has

$$H_{\pm(1/2)\pm 1} = \frac{2\sqrt{2}}{3}\mu_q \sin 2\theta \beta M_+ M_- \sqrt{\frac{M_2}{M_1}}. \quad (52)$$

For $\beta \equiv 1$ our helicity amplitudes coincide with the predictions of the NQM. We can also deduce the form factor F_2 [see the expression for the matrix element of the $1/2^+ \to 1/2^+$ transition (A2)]:

$$F_2 = -\frac{2}{3}\mu_q \sin 2\theta \beta M_1 \sqrt{\frac{M_2}{M_1}}. \quad (53)$$

Note that the form factor F_1 defined in (A2) vanishes due to gauge invariance. Finally the decay width for the $B_{bc}^h \to B_{bc}^l$ transition in the HQL reads

$$\Gamma(B_{bc}^h \to B_{bc}^l) = \frac{4}{3} K \mu_q^2 \sin^2 2\theta, \quad (54)$$

which again coincides with the prediction of the NQM [see Eq. (B12)] when $\beta \equiv 1$.

Note that in the HQL our model also reproduces the model-independent results derived in [11] for the decay rates involving mixed states $\frac{1}{2}^h$ and $\frac{1}{2}^l$:

$$\Gamma_{(1/2)^h \to (1/2)^l} \sim \mu_q^2 \sin^2 2\theta, \qquad \Gamma_{(3/2)\to(1/2)^l} \sim \mu_q^2 \cos^2\theta,$$
$$\Gamma_{(3/2)\to(1/2)^h} \sim \mu_q^2 \sin^2\theta, \qquad \frac{\Gamma_{(3/2)\to(1/2)^h}}{\Gamma_{(3/2)\to(1/2)^l}} \sim \tan^2\theta. \quad (55)$$

V. RESULTS

We now proceed to present our numerical results. We first present results on the radiative rates using finite heavy quark masses; i.e. we do not take the HQL for the matrix elements. Estimates for the decay widths are also given for the nonrelativistic quark model, in which, as described before, the wave functions have the same spin-flavor structure as our relativistic current considered in the nonrelativistic limit. Then we consider the HQL in both approaches. We choose the Gaussian form of Eq. (20) for the correlation function of the double-heavy baryons. Our results depend on the following set of parameters: the constituent quark masses and the size parameter Λ_B. The parameters have been taken from a fit to the properties of light, single, and double-heavy baryons in previous analyses [15]:

$m_{u(d)}$	m_s	m_c	m_b	Λ_B	
0.42	0.57	1.7	5.2	2.5–3.5	GeV.

(56)

All our analytical calculations have been done using the computer program FORM [27].

In Table III we present detailed numerical results on the radiative rates of double-heavy baryons using finite masses for the heavy quarks (exact results, second column) and in the HQL (third column). These are compared to the corresponding results of the NQM using finite masses for the heavy quarks (fourth column). In column 5 we take the

TABLE III. Radiative decay widths of DHBs in keV.

Decay mode	Exact results	HQL	NQM	NQM + HQL
$\Xi_{bc}^{l+} \to \Xi_{bc}^{+}$	$(1.56 \pm 0.08) \times 10^{-2}$	0	1.35×10^{-2}	0
$\Xi_{bc}^{l0} \to \Xi_{bc}^{0}$	$(1.56 \pm 0.08) \times 10^{-2}$	0	1.35×10^{-2}	0
$\Omega_{bc}^{l} \to \Omega_{bc}$	$(1.26 \pm 0.05) \times 10^{-2}$	0	1.10×10^{-2}	0
$\Xi_{bc}^{h+} \to \Xi_{bc}^{l+}$	0.14 ± 0.03	$\simeq 0.17$	0.34	0.53
$\Xi_{bc}^{h0} \to \Xi_{bc}^{l0}$	0.31 ± 0.04	$\simeq 0.04$	0.26	0.13
$\Omega_{bc}^{h} \to \Omega_{bc}^{l}$	0.21 ± 0.02	$\simeq 0.02$	0.15	0.06
$\Xi_{bc}^{*+} \to \Xi_{bc}^{l+}$	$(0.28 \pm 0.01) \times 10^{-2}$	0	0.25×10^{-2}	0
$\Xi_{bc}^{*0} \to \Xi_{bc}^{l0}$	$(0.28 \pm 0.01) \times 10^{-2}$	0	0.25×10^{-2}	0
$\Omega_{bc}^{*} \to \Omega_{bc}^{l}$	$(0.16 \pm 0.01) \times 10^{-2}$	0	0.14×10^{-2}	0
$\Xi_{cc}^{*++} \to \Xi_{cc}^{++}$	23.46 ± 3.33	20.53 ± 0.79	36.22	63.88
$\Xi_{cc}^{*+} \to \Xi_{cc}^{+}$	28.79 ± 2.51	5.13 ± 0.20	35.65	15.97
$\Omega_{cc}^{*} \to \Omega_{cc}$	2.11 ± 0.11	$\simeq 0.29$	2.42	0.87
$\Xi_{bc}^{*+} \to \Xi_{bc}^{+}$	0.49 ± 0.09	$\simeq 0.27$	0.67	0.83
$\Xi_{bc}^{*0} \to \Xi_{bc}^{0}$	0.24 ± 0.04	$\simeq 0.07$	0.30	0.21
$\Omega_{bc}^{*} \to \Omega_{bc}$	0.12 ± 0.02	$\simeq 0.03$	0.13	0.08
$\Xi_{bc}^{*+} \to \Xi_{bc}^{l+}$	0.46 ± 0.10	$\simeq 0.37$	0.69	1.14
$\Xi_{bc}^{*+} \to \Xi_{bc}^{h+}$	$(0.15 \pm 0.02) \times 10^{-2}$	$\simeq 0.03 \times 10^{-2}$	0.16×10^{-2}	0.08×10^{-2}
$\Xi_{bc}^{*0} \to \Xi_{bc}^{l0}$	0.51 ± 0.06	$\simeq 0.10$	0.59	0.28
$\Xi_{bc}^{*0} \to \Xi_{bc}^{h0}$	$(0.02 \pm 0.02) \times 10^{-4}$	$\simeq 0.06 \times 10^{-3}$	0.01×10^{-3}	0.19×10^{-3}
$\Omega_{bc}^{*} \to \Omega_{bc}^{l}$	(0.29 ± 0.03)	$\simeq 0.03$	0.30	0.12
$\Omega_{bc}^{*} \to \Omega_{bc}^{h}$	$(0.01 \pm 0.01) \times 10^{-4}$	$\simeq 0.01 \times 10^{-3}$	0.01×10^{-4}	0.03×10^{-3}
$\Xi_{bb}^{*0} \to \Xi_{bb}^{0}$	0.31 ± 0.06	$\simeq 0.11$	0.38	0.35
$\Xi_{bb}^{*-} \to \Xi_{bb}^{-}$	$(5.87 \pm 1.42) \times 10^{-2}$	$\simeq 2.8 \times 10^{-2}$	7.34×10^{-2}	8.69×10^{-2}
$\Omega_{bb}^{*} \to \Omega_{bb}$	$(2.26 \pm 0.45) \times 10^{-2}$	$\simeq 1.0 \times 10^{-2}$	2.36×10^{-2}	2.97×10^{-2}

heavy quark limit of the NQM results by setting the heavy quark magnetic moments to zero. The dependence of our results on the size parameter Λ_B is indicated by error bars where the variation of Λ_B is given in Eq. (56). Note that a smaller value of Λ gives bigger rates and vice versa. One can see that our finite heavy quark mass predictions are close to the results of the NQM. One has to keep in mind that the rate predictions are very sensitive to the mass difference $\Delta M = M_1 - M_2$. In fact, one has $\Gamma \sim (\Delta M)^3$ (see Appendix B). The modes involving mixed states are enhanced by factors $\simeq 4$ and $\simeq 2$ in the case of $B_{bc}^h \to B_{bc}^l$ and $B_{bc}^* \to B_{bc}^l$ transitions, respectively, while in the case of $B_{bc}^* \to B_{bc}^h$ transitions they are additionally suppressed by a factor $\simeq 10$ due to reduction of the mass difference $M_1 - M_2$. In Table IV we present results for the rates involving mixed states in dependence on the mixing angle θ_B varied from 10° to 25°. In Table V we compare our results with the results of a nonrelativistic quark model calculation [17]. The approach [17] can be viewed as an extension of the naive NQM discussed before by taking into account baryon wave functions in configuration space. One should emphasize that the results of nonrelativistic quark models are in general frame-dependent. For example, the results can depend on whether one works in the parent baryon or daughter baryon rest frame. Also, it is difficult to maintain gauge invariance in nonrelativistic quark models.

One final remark concerns the comparison of radiative and weak decays of DHBs. In [3] we have calculated the $b \to c$ semileptonic decays where we have shown that the corresponding decay widths are of the order of 10^{-14} GeV. The radiative decay widths calculated in the present paper

TABLE IV. θ_B dependence of radiative decay widths involving mixed DHBs in eV.

θ_B	Decay mode	Exact results	HQL	NQM	NQM + HQL
10°	$\Xi_{bc}^{h+} \to \Xi_{bc}^{l+}$	0.2 ± 0.2	$\simeq 10$	3	31
	$\Xi_{bc}^{h0} \to \Xi_{bc}^{l0}$	170 ± 15	$\simeq 3$	43	8
	$\Omega_{bc}^{h} \to \Omega_{bc}^{l}$	130 ± 10	$\simeq 1$	28	3
	$\Xi_{bc}^{*+} \to \Xi_{bc}^{h+}$	0.07 ± 0.01	$\simeq 0.3$	5	1
	$\Xi_{bc}^{*0} \to \Xi_{bc}^{h0}$	$\simeq 0.1$	$\simeq 0.1$	0.7	0.3
	$\Omega_{bc}^{*} \to \Omega_{bc}^{h}$	$\simeq 0.03$	$\simeq 0.02$	0.5	0.1
	$\Xi_{bc}^{*+} \to \Xi_{bc}^{l+}$	687 ± 132	276 ± 11	626	859
	$\Xi_{bc}^{*0} \to \Xi_{bc}^{l0}$	475 ± 65	69 ± 3	360	215
	$\Omega_{bc}^{*} \to \Omega_{bc}^{l}$	263 ± 26	$\simeq 28$	164	84
15°	$\Xi_{bc}^{h+} \to \Xi_{bc}^{l+}$	16 ± 7	27 ± 1	27	84
	$\Xi_{bc}^{h0} \to \Xi_{bc}^{l0}$	224 ± 24	$\simeq 7$	73	21
	$\Omega_{bc}^{h} \to \Omega_{bc}^{l}$	166 ± 14	$\simeq 3$	44	9
	$\Xi_{bc}^{*+} \to \Xi_{bc}^{h+}$	0.9 ± 0.1	$\simeq 0.6$	6	2
	$\Xi_{bc}^{*0} \to \Xi_{bc}^{h0}$	$\simeq 0.05$	$\simeq 0.1$	0.2	0.5
	$\Omega_{bc}^{*} \to \Omega_{bc}^{h}$	$\simeq 0.02$	$\simeq 0.1$	0.2	0.1
	$\Xi_{bc}^{*+} \to \Xi_{bc}^{l+}$	619 ± 122	289 ± 12	619	900
	$\Xi_{bc}^{*0} \to \Xi_{bc}^{l0}$	493 ± 66	72 ± 3	404	225
	$\Omega_{bc}^{*} \to \Omega_{bc}^{l}$	276 ± 26	$\simeq 29$	187	88
20°	$\Xi_{bc}^{h+} \to \Xi_{bc}^{l+}$	63 ± 19	64 ± 2	100	200
	$\Xi_{bc}^{h0} \to \Xi_{bc}^{l0}$	272 ± 31	16 ± 1	126	51
	$\Omega_{bc}^{h} \to \Omega_{bc}^{l}$	195 ± 17	$\simeq 7.3$	72	22
	$\Xi_{bc}^{*+} \to \Xi_{bc}^{h+}$	1.2 ± 0.1	$\simeq 1.5$	5	2
	$\Xi_{bc}^{*0} \to \Xi_{bc}^{h0}$	$\simeq 0.01$	$\simeq 0.2$	0.01	0.5
	$\Omega_{bc}^{*} \to \Omega_{bc}^{h}$	$\simeq 0.01$	$\simeq 0.03$	0.03	0.1
	$\Xi_{bc}^{*+} \to \Xi_{bc}^{l+}$	546 ± 111	313 ± 12	632	973
	$\Xi_{bc}^{*0} \to \Xi_{bc}^{l0}$	504 ± 65	78 ± 3	468	243
	$\Omega_{bc}^{*} \to \Omega_{bc}^{l}$	286 ± 27	$\simeq 32$	223	96
25°	$\Xi_{bc}^{h+} \to \Xi_{bc}^{l+}$	135 ± 34	91 ± 4	177	284
	$\Xi_{bc}^{h0} \to \Xi_{bc}^{l0}$	306 ± 37	223 ± 1	142	71
	$\Omega_{bc}^{h} \to \Omega_{bc}^{l}$	213 ± 20	$\simeq 18$	131	52
	$\Xi_{bc}^{*+} \to \Xi_{bc}^{h+}$	1.4 ± 0.2	$\simeq 0.3$	2	1
	$\Xi_{bc}^{*0} \to \Xi_{bc}^{h0}$	0.001 ± 0.001	$\simeq 0.08$	0.004	0.2
	$\Omega_{bc}^{*} \to \Omega_{bc}^{h}$	0.001 ± 0.001	$\simeq 0.02$	0.002	0.04
	$\Xi_{bc}^{*+} \to \Xi_{bc}^{l+}$	469 ± 99	373 ± 15	680	1115
	$\Xi_{bc}^{*0} \to \Xi_{bc}^{l0}$	507 ± 64	90 ± 3	578	278
	$\Omega_{bc}^{*} \to \Omega_{bc}^{l}$	291 ± 26	$\simeq 37$	281	111

TABLE V. Radiative decay widths of DHBs in keV. Comparison with the quark model [17].

Decay mode	Quark model [17]	Our results
$\Xi_{bc}^{\prime+} \to \Xi_{bc}^{+}$	0.992×10^{-2}	$(1.56 \pm 0.08) \times 10^{-2}$
$\Xi_{bc}^{\prime 0} \to \Xi_{bc}^{0}$	0.992×10^{-2}	$(1.56 \pm 0.08) \times 10^{-2}$
$\Omega_{bc}^{\prime} \to \Omega_{bc}$	3.69×10^{-2}	$(1.26 \pm 0.05) \times 10^{-2}$
$\Xi_{bc}^{h+} \to \Xi_{bc}^{\prime+}$	12.4×10^{-2}	$(14 \pm 4) \times 10^{-2}$
$\Xi_{bc}^{h0} \to \Xi_{bc}^{\prime 0}$	20.9×10^{-2}	$(31 \pm 4) \times 10^{-2}$
$\Omega_{bc}^{h} \to \Omega_{bc}^{\prime}$	8.52×10^{-2}	$(21 \pm 2) \times 10^{-2}$
$\Xi_{bc}^{*+} \to \Xi_{bc}^{\prime+}$	4.04×10^{-2}	$(0.28 \pm 0.01) \times 10^{-2}$
$\Xi_{bc}^{*0} \to \Xi_{bc}^{\prime 0}$	4.04×10^{-2}	$(0.28 \pm 0.01) \times 10^{-2}$
$\Omega_{bc}^{*} \to \Omega_{bc}^{\prime}$	3.69×10^{-2}	$(0.16 \pm 0.01) \times 10^{-2}$
$\Xi_{bc}^{*+} \to \Xi_{bc}^{+}$	1.05	0.49 ± 0.09
$\Xi_{bc}^{*0} \to \Xi_{bc}^{0}$	0.505	0.24 ± 0.04
$\Omega_{bc}^{*} \to \Omega_{bc}$	0.209	0.12 ± 0.02
$\Xi_{bc}^{*+} \to \Xi_{bc}^{\prime+}$	0.739	0.46 ± 0.10
$\Xi_{bc}^{*+} \to \Xi_{bc}^{h+}$	6.05×10^{-2}	$(0.15 \pm 0.02) \times 10^{-2}$
$\Xi_{bc}^{*0} \to \Xi_{bc}^{\prime 0}$	1.03	0.51 ± 0.06
$\Xi_{bc}^{*0} \to \Xi_{bc}^{h0}$	0.12×10^{-2}	$(0.02 \pm 0.02) \times 10^{-2}$
$\Omega_{bc}^{*} \to \Omega_{bc}^{\prime}$	0.502	0.29 ± 0.03
$\Omega_{bc}^{*} \to \Omega_{bc}^{h}$	0.31×10^{-2}	$(0.01 \pm 0.01) \times 10^{-4}$

are much larger and lie in the range from 10^{-8} to 10^{-4} GeV. One would like to know how important the weak decays of DHBs induced by the $q_i \to q_j$ ($d \to u$ or $s \to u$) light quark transitions are. For a precise analysis one would need to know the precise values of the masses of the DHBs including isospin-breaking corrections which are not available at present. Instead using the general formula for the semileptonic decay width one can obtain a rough estimate for the decay rates induced by light quark transitions where, for the sake of simplicity, we neglect the contribution of form factors, spin, and flavor factors. For example, for the $1/2^+ \to 1/2^+$ transition one obtains (see e.g. [28])

$$\Gamma(q_i \to q_j) \cong \frac{G_F^2 |V_{\mathrm{CKM}}|^2}{15\pi^3} \Delta M^5, \tag{57}$$

where $G_F = 1.166\,34 \times 10^{-5}$ GeV^{-2} is the Fermi constant, V_{CKM} is CKM matrix element ($|V_{ud}|^2 \simeq 1$ and $|V_{us}|^2 = 0.051$), and $\Delta M = M_1 - M_2$ is the difference of the masses of initial and final baryons. We know from data on the mass differences of light and heavy-light baryons that, approximately, the mass difference ΔM does not exceed the mass difference of the corresponding light quarks in these baryons. Therefore, in the expression for $\Gamma(q_i \to q_j)$ we substitute $\Delta M \le m_d - m_u$ for $d \to u$ transitions and $\Delta M \le m_s - m_u$ for $s \to u$ transitions and consider this to be an approximation of the upper limit for the corresponding decay rates. Using upper limits $m_d - m_u < 10$ MeV and $m_s - m_u < 200$ MeV we obtain

$$\Gamma(d \to u) < 10^{-22}\ \mathrm{GeV}, \qquad \Gamma(s \to u) < 10^{-18}\ \mathrm{GeV}. \tag{58}$$

Based on this rough estimate one concludes that the semileptonic decays of DHBs induced by the light quark transitions $d \to u$ and $s \to u$ are suppressed by more than 4 orders of magnitude in comparison to their $b \to c$ counterparts and are even more suppressed (more than 10 orders) compared to their radiative decays.

VI. SUMMARY

We have analyzed the radiative decays of double-heavy baryons using a manifestly Lorentz covariant and gauge-invariant constituent quark model approach. Our main results can be summarized as follows. We have derived results for the radiative transition matrix elements of double-heavy baryons for finite values of the heavy quark/baryon masses and also in the HQL limit of infinitely heavy quark masses. We have discussed in detail radiative transitions involving DHB states subject to hyperfine mixing. We have presented an extensive numerical analysis of the decay rates for finite masses and in the HQL limit including numerical results on mixing effects. Our results were compared with the predictions of a nonrelativistic quark model including again hyperfine mixing effects. We find that the inclusion of hyperfine mixing effects has a profound influence on the pattern of radiative decays of DHBs. Since the calculated rates depend very sensitively on the exact mass values of the mixed and unmixed DHB states [$\Gamma \sim (M_1 - M_2)^3$] one must wait for an accurate determination of the masses of the DHB states before one can extract information on the mixing angles from the decay data.

ACKNOWLEDGMENTS

This work was supported by the DFG under Contract No. FA67/31-2 and No. GRK683. M. A. I. appreciates the partial support by DFG Grant No. KO 1069/13-1, the Heisenberg-Landau program, and Russian Fund of Basic Research Grant No. 10-02-00368-a. This research is also part of the European Community-Research Infrastructure Integrating Activity "Study of Strongly Interacting Matter" (acronym HadronPhysics2, Grant Agreement No. 227431), Russian President Grant "Scientific Schools" No. 3400.2010.2, and Russian Science and Innovations Federal Agency Contract No. 02.740.11.0238.

APPENDIX A: SPIN KINEMATICS OF RADIATIVE DECAYS

In this appendix we write down covariant expansions for the current-induced electromagnetic transitions involving the $(1/2^+)$ and $(3/2^+)$ baryon states. We thereby define sets of invariant vector transition form factors. We then define helicity amplitudes which are expressed in terms of linear combinations of the invariant form factors. One of the advantages of using helicity amplitudes is that one obtains very compact expressions for the decay rates (see

e.g. [28,29]). In addition, the helicity amplitudes contain the complete spin information of the process and are thus well suited for the computation of spin observables.

In the radiative decays of double-heavy baryons the momenta and masses are denoted by

$$B_1(p_1, M_1) \to B_2(p_2, M_2) + \gamma(q), \tag{A1}$$

where $p_1 = p_2 + q$. For the invariant form factor expansion of the $1/2^+ \to 1/2^+$ matrix elements of the vector current J_μ one obtains the following.

Transition $\frac{1}{2} \to \frac{1}{2} + +$:

$$\begin{aligned} M_\mu &= \langle B_2|J_\mu|B_1\rangle \\ &= \bar{u}(p_2, s_2)\Big[\gamma_\mu F_1(q^2) - i\sigma_{\mu\nu}\frac{q_\nu}{M_1}F_2(q^2) \\ &\quad + \frac{q_\mu}{M_1}F_3(q^2)\Big]u(p_1, s_1). \end{aligned} \tag{A2}$$

Similarly one has

Transition $\frac{3}{2}^+ \to \frac{1}{2}^+$:

$$\begin{aligned} M_\mu &= \langle B_2|J_\mu|B_1^*\rangle \\ &= \bar{u}(p_2, s_2)\Big[g_{\alpha\mu}F_1(q^2) + \gamma_\mu\frac{p_{2\alpha}}{M_2}F_2(q^2) \\ &\quad + \frac{p_{2\alpha}p_{1\mu}}{M_2^2}F_3(q^2) + \frac{p_{2\alpha}q_\mu}{M_2^2}F_4(q^2)\Big]\gamma_5 u^\alpha(p_1, s_1), \end{aligned} \tag{A3}$$

where $\sigma_{\mu\nu} = (i/2)(\gamma_\mu\gamma_\nu - \gamma_\nu\gamma_\mu)$ and all γ matrices are defined as in Bjorken-Drell. One should emphasize that the above invariant form factors are constrained by gauge invariance relations (see e.g. the detailed discussion in [30]).

Next we express the vector helicity amplitudes $H_{\lambda_2\lambda_\gamma}$ in terms of the invariant form factors F_i, where $\lambda_\gamma = \pm 1$ and $\lambda_2 = \pm 1/2$ and $\pm 3/2$ are the helicity components of the on-shell photon and the daughter baryon, respectively. The pertinent relation is

$$H_{\lambda_2\lambda_\gamma} = M_\mu(\lambda_2)\bar{\epsilon}^{*\mu}(\lambda_\gamma). \tag{A4}$$

Angular momentum conservation fixes the helicity λ_1 of the parent baryon according to $\lambda_1 = \lambda_2 - \lambda_\gamma$. We shall work in the rest frame of the parent baryon B_1 with the daughter baryon B_2 moving in the positive z direction such that $p_1^\mu = (M_1, \mathbf{0})$, $p_2^\mu = (E_2, 0, 0, |\mathbf{p}_2|)$ and $q^\mu = (q_0, 0, 0, -|\mathbf{p}_2|)$, where $q_0 = |\mathbf{p}_2| = (M_1^2 - M_2^2)/(2M_1)$ and $E_2 = M_1 - q_0 = (M_1^2 + M_2^2)/(2M_1)$.

The $J = \frac{1}{2}$ baryon spinors are given by

$$\begin{aligned} \bar{u}_2\Big(p_2, \pm\frac{1}{2}\Big) &= \sqrt{E_2 + M_2}\Big(\chi_\pm^\dagger, \frac{\mp|\mathbf{p}_2|}{E_2 + M_2}\chi_\pm^\dagger\Big), \\ u_1\Big(p_1, \pm\frac{1}{2}\Big) &= \sqrt{2M_1}\begin{pmatrix}\chi_\pm \\ 0\end{pmatrix}, \end{aligned} \tag{A5}$$

where

$$\chi_+ = \begin{pmatrix}1 \\ 0\end{pmatrix}$$

and

$$\chi_- = \begin{pmatrix}0 \\ 1\end{pmatrix}$$

are two-component Pauli spinors.

The $J = \frac{3}{2}$ baryon spinors are defined by

$$u_\mu(p, s^*) = \sum_{\lambda, s}\Big\langle 1\lambda\frac{1}{2}s\,\Big|\,\frac{3}{2}s^*\Big\rangle\epsilon_\mu(p, \lambda)u(p, s). \tag{A6}$$

They satisfy the Rarita-Schwinger conditions

$$\gamma^\mu u_\mu(p, s^*) = p^\mu u_\mu(p, s^*) = 0, \tag{A7}$$

where $\langle 1\lambda\frac{1}{2}s|\frac{3}{2}s^*\rangle$ is the requisite Clebsch-Gordan coefficient, $\epsilon_\mu(p, \lambda)$ is the spin 1 polarization vector, and $u(p, s)$ are the usual $J = \frac{1}{2}$ spinors defined above. In particular, the $J = \frac{3}{2}$ spinors with helicities $\lambda = \pm 3/2, \pm 1/2$ read

$$\begin{aligned} u_\mu\Big(p, \pm\frac{3}{2}\Big) &= \epsilon_\mu(p, \pm 1)u\Big(p, \pm\frac{1}{2}\Big), \\ u_\mu\Big(p, \pm\frac{1}{2}\Big) &= \sqrt{\frac{2}{3}}\epsilon_\mu(p, 0)u\Big(p, \pm\frac{1}{2}\Big) \\ &\quad + \sqrt{\frac{1}{3}}\epsilon_\mu(p, \pm 1)u\Big(p, \mp\frac{1}{2}\Big). \end{aligned} \tag{A8}$$

The polarization vectors corresponding to the parent and daughter $J = \frac{3}{2}$ baryons are given by

$$\begin{aligned} \epsilon^\mu(p_1, 0) &= (0, 0, 0, 1), \\ \epsilon^\mu(p_1, \pm 1) &= \frac{1}{\sqrt{2}}(0, \mp 1, -i, 0), \\ \epsilon^{*\mu}(p_2, 0) &= \frac{1}{M_2}(|\mathbf{p}_2|, 0, 0, E_2), \\ \epsilon^{*\mu}(p_2, \pm 1) &= \frac{1}{\sqrt{2}}(0, \mp 1, i, 0). \end{aligned} \tag{A9}$$

The polarization vectors of the on-shell photon read

$$\bar{\epsilon}^{*\mu}(\pm 1) = \frac{1}{\sqrt{2}}(0, \pm 1, i, 0), \tag{A10}$$

where the "bar" on the polarization vector denotes the fact that the photon is moving in the negative z direction. The polarization vectors satisfy the Lorentz condition

$$q_\mu\bar{\epsilon}^{*\mu}(\pm 1) = 0. \tag{A11}$$

Using above formulas for the spin wave functions with definite helicities one can then express the helicity amplitudes $H_{\lambda_2\lambda_\gamma}$ through the invariant form factors by calculating $H_{\lambda_2\lambda_\gamma} = M_\mu(\lambda_2)\bar{\epsilon}^{*\mu}(\lambda_\gamma)$. One obtains the following.

Transition $\frac{1}{2}^+ \to \frac{1}{2}^+$:

$$H_{\pm(1/2)\pm 1} = -F_2\sqrt{2}\frac{M_+M_-}{M_1}, \tag{A12}$$

where $M_\pm = M_1 \pm M_2$.

Transition $\frac{3}{2}^+ \to \frac{1}{2}^+$:

$$\begin{aligned} H_{\pm(1/2)\pm 1} &= \pm\frac{1}{\sqrt{3}}M_-\left(F_1 + F_2\frac{M_+^2}{M_1M_2}\right), \\ H_{\pm(1/2)\mp 1} &= \pm M_- F_1. \end{aligned} \tag{A13}$$

Note that one has an explicit factor of M_- in all the helicity amplitudes which corresponds to the appropriate p-wave threshold factor $|\mathbf{p}| \sim M_-$. The decay width is given by

$$\Gamma_{s_1\to s_2} = \frac{\alpha}{2s_1+1}\frac{M_1^2 - M_2^2}{4M_1^3}\mathcal{H}_{s_1\to s_2}, \tag{A14}$$

where the $\mathcal{H}_{s_1\to s_2}$ are bilinear combinations of the helicity amplitudes:

$$\begin{aligned} \mathcal{H}_{(1/2)\to(1/2)} &= |H_{(1/2)1}|^2 + |H_{-(1/2)-1}|^2, \\ \mathcal{H}_{(3/2)\to(1/2)} &= |H_{(1/2)1}|^2 + |H_{-(1/2)-1}|^2 \\ &\quad + |H_{(1/2)-1}|^2 + |H_{-(1/2)1}|^2. \end{aligned} \tag{A15}$$

The overall dependence of the rate on the mass difference M_- can be seen to be given by $|\mathbf{p}|^{2l+1} \sim M_-^3$ for $l = 1$. In the HQL the baryon spinors simplify. For example, the HQL $J = \frac{1}{2}$ baryon spinors read

$$\begin{aligned} \bar{u}_2\left(v, \pm\frac{1}{2}\right) &= \sqrt{2M_2}(\chi_\pm^\dagger, 0), \\ u_1\left(v, \pm\frac{1}{2}\right) &= \sqrt{2M_1}\begin{pmatrix}\chi_\pm \\ 0\end{pmatrix}. \end{aligned} \tag{A16}$$

For the $\frac{3}{2}^+ \to \frac{1}{2}^+$ transition in the HQL one has four possible Dirac strings in the matrix elements which are γ_5, $\gamma_5 \not{v}$, $\gamma_5 \bar{\not{\epsilon}}^*(\lambda_\gamma)$, and $\gamma_5 \not{v}\bar{\not{\epsilon}}^*(\lambda_\gamma)$. It is easy to show that the two Dirac strings γ_5 and $\gamma_5 \not{v}\bar{\not{\epsilon}}^*(\lambda_\gamma)$ vanish when sandwiched between the HQL baryon spinors:

$$\begin{aligned} &\bar{u}_2(v, \pm\tfrac{1}{2})(\gamma_5, \gamma_5\not{v}\bar{\not{\epsilon}}^*(\lambda_\gamma))u_\mu(v, \pm\tfrac{3}{2}) \\ &\quad = \bar{u}_2(v, \pm\tfrac{1}{2})(\gamma_5, \gamma_5\not{v}\bar{\not{\epsilon}}^*(\lambda_\gamma))u_\mu(v, \mp\tfrac{1}{2}) = 0. \end{aligned} \tag{A17}$$

The remaining strings $\gamma_5 \not{q}$ and $\gamma_5 \bar{\not{\epsilon}}^*$ one has

$$\bar{u}_2\left(v, \pm\frac{1}{2}\right)\gamma_5\not{q}u_\mu\left(v, \pm\frac{3}{2}\right) = \mp M_+M_-\sqrt{\frac{M_2}{M_1}}\epsilon_\mu(v, \pm 1), \qquad \bar{u}_2\left(v, \pm\frac{1}{2}\right)\gamma_5\not{q}u_\mu\left(v, \mp\frac{1}{2}\right) = \mp\sqrt{\frac{1}{3}}M_+M_-\sqrt{\frac{M_2}{M_1}}\epsilon_\mu(v, \mp 1),$$
$$\bar{u}_2\left(v, \pm\frac{1}{2}\right)\gamma_5\bar{\not{\epsilon}}^*(\mp 1)u_\mu\left(v, \pm\frac{3}{2}\right) = 0, \qquad \bar{u}_2\left(v, \pm\frac{1}{2}\right)\gamma_5\bar{\epsilon}^*(\pm 1)u_\mu\left(v, \mp\frac{1}{2}\right) = \pm\frac{4}{\sqrt{3}}\sqrt{M_1M_2}\epsilon_\mu(v, 0). \tag{A18}$$

In the calculation of the helicity amplitudes $H_{\pm(1/2)\pm 1}$ and $H_{\pm(1/2)\mp 1}$ one can make use of the HQL identities

$$\begin{aligned} &\bar{u}_2\left(v, \pm\frac{1}{2}\right)\gamma_5\not{q}\bar{\epsilon}^{*\mu}(\mp 1)u_\mu\left(v, \pm\frac{3}{2}\right) = \sqrt{3}\bar{u}_2\left(v, \pm\frac{1}{2}\right)\gamma_5\not{q}\bar{\epsilon}^{*\mu}(\pm 1)u_\mu\left(v, \mp\frac{1}{2}\right) = \pm M_+M_-\sqrt{\frac{M_2}{M_1}}, \\ &\bar{u}_2\left(v, \pm\frac{1}{2}\right)\gamma_5\bar{\not{\epsilon}}^*(\pm 1)q^\mu u_\mu\left(v, \mp\frac{1}{2}\right) = \pm\frac{2}{\sqrt{3}}M_+M_-\sqrt{\frac{M_2}{M_1}}. \end{aligned} \tag{A19}$$

APPENDIX B: NONRELATIVISTIC QUARK MODEL: SPIN-FLAVOR WAVE FUNCTIONS, RADIATIVE DECAY CONSTANTS, AND WIDTHS OF DOUBLE-HEAVY BARYONS

In this appendix we present results on the radiative decay amplitudes and widths of the DHBs in the nonrelativistic quark model. As emphasized before the nonrelativistic quark model is based on the spin-flavor wave functions which arise in the nonrelativistic limit of the relativistically covariant double-heavy three-quark currents with quantum numbers $J^P = \frac{1}{2}^+$ and $\frac{3}{2}^+$. The corresponding quark model spin-flavor wave functions are given in Table II, where we use the following notation for the antisymmetric $\chi_A(\lambda)$ and symmetric $\chi_S(\lambda)$, $\chi_S^*(\lambda)$ spin wave functions where λ is the helicity of the baryon state:

$$\chi_A\left(\frac{1}{2}\right) = \sqrt{\frac{1}{2}}\{\uparrow(\uparrow\downarrow - \downarrow\uparrow)\}, \qquad \chi_A\left(-\frac{1}{2}\right) = \sqrt{\frac{1}{2}}\{\downarrow(\uparrow\downarrow - \downarrow\uparrow)\},$$
$$\chi_S\left(\frac{1}{2}\right) = \sqrt{\frac{1}{6}}\{2\downarrow\uparrow\uparrow - \uparrow(\uparrow\downarrow + \downarrow\uparrow)\}, \qquad \chi_S\left(-\frac{1}{2}\right) = -\sqrt{\frac{1}{6}}\{2\uparrow\downarrow\downarrow - \downarrow(\uparrow\downarrow + \downarrow\uparrow)\},$$
$$\chi_S^*\left(\frac{3}{2}\right) = \uparrow\uparrow\uparrow, \qquad \chi_S^*\left(-\frac{3}{2}\right) = \downarrow\downarrow\downarrow,$$
$$\chi_S^*\left(\frac{1}{2}\right) = \sqrt{\frac{1}{3}}\{\uparrow\uparrow\downarrow + \uparrow\downarrow\uparrow + \downarrow\uparrow\uparrow\}, \qquad \chi_S^*\left(-\frac{1}{2}\right) = \sqrt{\frac{1}{3}}\{\uparrow\downarrow\downarrow + \downarrow\uparrow\downarrow + \downarrow\downarrow\uparrow\}. \tag{B1}$$

In (B1) we use the ordering $\{qQ_1Q_2\}$. Next we relate the DHB radiative decay amplitudes to the nonrelativistic amplitudes $G_{\lambda_2\lambda_\gamma}$, where $\lambda_\gamma = \pm 1$ and $\lambda_2 = \pm 1/2$ and $\pm 3/2$ are the helicity components of the on-shell photon and the daughter baryon, respectively (see details in Appendix A). In order to evaluate the spin-flip matrix elements between the baryon states we make use of the spin-flip (spin raising/lowering) operator

$$\mathcal{S}^{\pm}_{\text{flip}} = -\sqrt{2}\sum_{i=1}^{3}\mu_i(\sigma_\pm)_i, \tag{B2}$$

where i runs over the three constituent quarks. The spin-flip matrix elements are given by

$$G_{\lambda_2\mp 1} = \langle B_2(\lambda_2)|\mathcal{S}^{\pm}_{\text{flip}}|B_1(\lambda_1)\rangle, \tag{B3}$$

where $\lambda_1 = \lambda_2 - \lambda_\gamma$ is the helicity of the parent baryon and $\sigma_\pm = \sigma_1 \pm i\sigma_2$. $\mu_i = e_i/(2m_i)$ is the ith quark magnetic moment and e_i and m_i are its charge and mass, respectively.

For the amplitude $G_{\lambda_2\lambda_\gamma}$ one obtains the following.

Transition $\frac{1}{2}^A \to \frac{1}{2}^S$:

$$G_{\pm(1/2)\pm 1} = -\sqrt{\frac{2}{3}}(\mu_c - \mu_b). \tag{B4}$$

Transition $\frac{3}{2} \to \frac{1}{2}^A$:

$$G_{\pm(1/2)\mp 1} = -\sqrt{3}G_{\pm(1/2)\pm 1} = \pm(\mu_c - \mu_b). \tag{B5}$$

Transition $\frac{3}{2} \to \frac{1}{2}^S$:

$$G_{\pm(1/2)\mp 1} = -\sqrt{3}G_{\pm(1/2)\pm 1} = \pm\frac{2}{\sqrt{3}}\left(\mu_q - \frac{\mu_{Q_1} + \mu_{Q_2}}{2}\right). \tag{B6}$$

Transition $\frac{1}{2}^h \to \frac{1}{2}^l$:

$$G_{\pm(1/2)\pm 1} = \frac{2\sqrt{2}}{3}\sin 2\theta_B\left(\mu_q - \frac{\sqrt{3}}{2}(\mu_c - \mu_b)\cot 2\theta_B\right). \tag{B7}$$

Transition $\frac{3}{2} \to \frac{1}{2}^l$:

$$G_{\pm(1/2)\mp 1} = -\sqrt{3}G_{\pm(1/2)\pm 1} = \pm\frac{2}{\sqrt{3}}\cos\theta_B\left(\mu_q - \frac{\mu_c}{2}\tan_+ - \frac{\mu_b}{2}\tan_-\right). \tag{B8}$$

Transition $\frac{3}{2} \to \frac{1}{2}^h$:

$$G_{\pm(1/2)\mp 1} = -\sqrt{3}G_{\pm(1/2)\pm 1} = \pm\frac{2}{\sqrt{3}}\sin\theta_B\left(\mu_q - \frac{\mu_c}{2}\cot_- - \frac{\mu_b}{2}\cot_+\right), \tag{B9}$$

where $\tan_\pm = 1 \pm \tan\theta_B\sqrt{3}$ and $\cot_\pm = 1 \pm \cot\theta_B\sqrt{3}$.

The states $\frac{1}{2}^A$, $\frac{1}{2}^S$, $\frac{1}{2}^l$, and $\frac{1}{2}^h$ correspond to baryons with antisymmetric, symmetric, and mixed heavy quark spin configuration, respectively. In particular, $\frac{1}{2}^h$ and $\frac{1}{2}^l$ correspond to the mixed states B_h and B_l. The index q corresponds to the light u, d, or s quark.

In terms of the nonrelativistic amplitude $G_{\lambda_2\lambda_\gamma}$ the helicity amplitudes $H_{\lambda_2\lambda_\gamma}$ (see details in Appendix A) for the $\frac{1}{2}^+ \to \frac{1}{2}^+$ and $\frac{3}{2}^+ \to \frac{1}{2}^+$ radiative transitions are defined by

$$H_{\lambda_2\lambda_\gamma} = |\mathbf{p}_2|\sqrt{N_1N_2}G_{\lambda_2\lambda_\gamma}, \tag{B10}$$

where $N_i = \sqrt{2M_i}$ is the extra factor acquired in the nonrelativistic quark model due to different normalization of states in the relativistic and the nonrelativistic theory. Therefore, we have

$$H_{\lambda_2\lambda_\gamma} = M_+M_-\sqrt{\frac{M_2}{M_1}}G_{\lambda_2\lambda_\gamma}. \tag{B11}$$

The radiative decay widths for the four possible $s_1 \to s_2$ spin transitions are given by

$$\Gamma_{(1/2)^A\to(1/2)^S} = \Gamma_{(3/2)\to(1/2)^A} = K\mu_c^2\left(1 - \frac{\mu_b}{\mu_c}\right)^2,$$
$$\Gamma_{(1/2)^h\to(1/2)^l} = \frac{4}{3}K\mu_q^2\sin^2 2\theta_B\left(1 - \frac{\sqrt{3}}{2}\frac{\mu_c - \mu_b}{\mu_q}\cot 2\theta_B\right)^2,$$
$$\Gamma_{(3/2)\to(1/2)^S} = \frac{4}{3}K\mu_q^2\left(1 - \frac{\mu_{Q_1} + \mu_{Q_1}}{2\mu_q}\right)^2,$$
$$\Gamma_{(3/2)\to(1/2)^l} = \frac{4}{3}K\mu_q^2\cos^2\theta_B\left(1 - \frac{\mu_c}{2\mu_q}\tan_+ - \frac{\mu_b}{2\mu_q}\tan_-\right)^2,$$
$$\Gamma_{(3/2)\to(1/2)^h} = \frac{4}{3}K\mu_q^2\sin^2\theta_B\left(1 - \frac{\mu_c}{2\mu_q}\cot_- - \frac{\mu_b}{2\mu_q}\cot_+\right)^2, \tag{B12}$$

where

$$K = \alpha M_2 \frac{(M_1^2 - M_2^2)^3}{6M_1^4} \tag{B13}$$

and $\alpha \simeq 1/137$ is the fine-structure constant.

It is evident that the widths of the subleading processes $\frac{1}{2}^A \to \frac{1}{2}^S$ and $\frac{3}{2} \to \frac{1}{2}^A$ are suppressed by a factor of $(m_q/m_c)^2$ compared to the widths of the leading process $\frac{3}{2} \to \frac{1}{2}^S$.

APPENDIX C: MASS OPERATOR AND RADIATIVE VERTEX FUNCTIONS OF DOUBLE-HEAVY BARYONS

The baryon mass operators $\Sigma_B(p)$ and $\Sigma_{B^*}^{\mu\nu}(p)$ are given by

$$\Sigma_B(p) = 6N_f \int dk_{123} \Phi^2(z_0) R_\Sigma(k_1^+, k_2^+, k_3^+),$$
$$R_\Sigma(r_1, r_2, r_3) = \Gamma_{1f} \tilde{S}_q(r_3) \bar{\Gamma}_{1i} \mathrm{tr}[\Gamma_{2f} \tilde{S}_{Q_2}(r_2) \bar{\Gamma}_{2i} \tilde{S}_{Q_1}(-r_1)], \tag{C1}$$

$$\Sigma_{B^*}^{\mu\nu}(p) = 6 \int dk_{123} \Phi^2(z_0) R_\Sigma^{\mu\nu}(k_1^+, k_2^+, k_3^+),$$
$$R_\Sigma^{\mu\nu}(r_1, r_2, r_3) = \Gamma_{1f} \tilde{S}_q(r_3) \bar{\Gamma}_{1i} \mathrm{tr}[\Gamma_{2f}^\mu \tilde{S}_{Q_2}(r_2) \bar{\Gamma}_{2i}^\nu \tilde{S}_{Q_1}(-r_1)]. \tag{C2}$$

Here and in the following N_f denotes a statistical flavor factor, which is equal to 1 or 2 for DHBs with two different or two identical heavy quarks, respectively, and $\bar{\Gamma} = \gamma^0 \Gamma^\dagger \gamma^0$. We have introduced the abbreviations

$$\begin{aligned}
dk_{123} &= \frac{d^4k_1 d^4k_2 d^4k_3}{(2\pi)^8 i^2} \delta^4(k_1 + k_2 + k_3), \\
z_0 &= -\frac{1}{3}(k_1^2 + k_2^2 + k_3^2), \qquad k_i^+ = k_i + p w_i, \\
k_i'^+ &= k_i + p' w_i, \qquad L_i = \frac{2}{3}\Big(k_i - \sum_{j=1}^3 k_j w_j\Big), \\
z_1(q) &= L_1 q - \frac{2}{3} q^2 (w_2^2 + w_2 w_3 + w_3^2), \\
z_2(q) &= L_2 q - \frac{2}{3} q^2 (w_1^2 + w_1 w_3 + w_3^2), \\
z_3(q) &= L_3 q - \frac{2}{3} q^2 (w_1^2 + w_1 w_2 + w_2^2),
\end{aligned} \tag{C3}$$

and

$$\begin{aligned}
R_{\mu,\Delta_1}^\perp(r_1, r_2, r_3, q) &= -\Gamma_{1f} \tilde{S}_q(r_3) \bar{\Gamma}_{1i} \mathrm{tr}[\Gamma_{2f} \tilde{S}_{Q_2}(r_2) \bar{\Gamma}_{2i} \tilde{S}_{Q_1}(-r_1) \gamma_\mu^\perp \tilde{S}_{Q_1}(-r_1 + q)], \\
R_{\mu,\Delta_2}^\perp(r_1, r_2, r_3, q) &= \Gamma_{1f} \tilde{S}_q(r_3) \bar{\Gamma}_{1i} \mathrm{tr}[\Gamma_{2f} \tilde{S}_{Q_2}(r_2 - q) \gamma_\mu^\perp \tilde{S}_{Q_2}(r_2) \bar{\Gamma}_{2i} \tilde{S}_{Q_1}(-r_1)], \\
R_{\mu,\Delta_3}^\perp(r_1, r_2, r_3, q) &= \Gamma_{1f} \tilde{S}_q(r_3 - q) \gamma_\mu^\perp \tilde{S}_q(r_3) \bar{\Gamma}_{1i} \mathrm{tr}[\Gamma_{2f} \tilde{S}_{Q_2}(r_2) \bar{\Gamma}_{2i} \tilde{S}_{Q_1}(-r_1)], \\
R_{\mu\nu,\Delta_1}^\perp(r_1, r_2, r_3, q) &= -\Gamma_{1f} \tilde{S}_q(r_3) \bar{\Gamma}_{1i} \mathrm{tr}[\Gamma_{2f} \tilde{S}_{Q_2}(r_2) \bar{\Gamma}_{2i,\nu} \tilde{S}_{Q_1}(-r_1) \gamma_\mu^\perp \tilde{S}_{Q_1}(-r_1 + q)], \\
R_{\mu\nu,\Delta_2}^\perp(r_1, r_2, r_3, q) &= \Gamma_{1f} \tilde{S}_q(r_3) \bar{\Gamma}_{1i} \mathrm{tr}[\Gamma_{2f} \tilde{S}_{Q_2}(r_2 - q) \gamma_\mu^\perp \tilde{S}_{Q_2}(r_2) \bar{\Gamma}_{2i,\nu} \tilde{S}_{Q_1}(-r_1)], \\
R_{\mu\nu,\Delta_3}^\perp(r_1, r_2, r_3, q) &= \Gamma_{1f} \tilde{S}_q(r_3 - q) \gamma_\mu^\perp \tilde{S}_q(r_3) \bar{\Gamma}_{1i} \mathrm{tr}[\Gamma_{2f} \tilde{S}_{Q_2}(r_2) \bar{\Gamma}_{2i,\nu} \tilde{S}_{Q_1}(-r_1)], \\
R_{\nu,\Sigma}(r_1, r_2, r_3) &= \Gamma_{1f} \tilde{S}_q(r_3) \bar{\Gamma}_{1i} \mathrm{tr}[\Gamma_{2f} \tilde{S}_{Q_2}(r_2) \bar{\Gamma}_{2i,\nu} \tilde{S}_{Q_1}(-r_1)].
\end{aligned} \tag{C4}$$

In the following we present explicit expressions for the electromagnetic vertex function. In case of the $(\frac{1}{2}^+, 0) \to (\frac{1}{2}^+, 1)$ and $(\frac{3}{2}^+, 1) \to (\frac{1}{2}^+, 0)$ transitions the expressions for the nonvanishing contribution of the triangle diagrams in Fig. 2(a)–2(c) (terms $\Lambda_{\mu,\Delta}^\perp$ and $\Lambda_{\mu\nu,\Delta}^\perp$, respectively) read

$$\Lambda_{\mu,\Delta}^\perp(p_1, p_2) = 6N_f g_{B_1} g_{B_2} \int dk_{123} \sum_{i=1}^3 e_i \Phi(z_0) \Phi(z_0 + z_i(q)) R_{\mu,\Delta_i}^\perp(k_1^+, k_2^+, k_3^+, q), \tag{C5a}$$

$$\Lambda_{\mu\nu,\Delta}^\perp(p_1, p_2) = 6N_f g_{B_1^*} g_{B_2} \int dk_{123} \sum_{i=1}^3 e_i \Phi(z_0) \Phi(z_0 + z_i(q)) R_{\mu\nu,\Delta_i}^\perp(k_1^+, k_2^+, k_3^+, q), \tag{C5b}$$

where $e_1 = e_{Q_1}$, $e_2 = e_{Q_2}$ and $e_3 = e_q$. For the $(\frac{3}{2}^+, 1) \to (\frac{1}{2}^+, 1)$ transition the electromagnetic vertex function $\Lambda_{\mu\nu}$ obtains contributions from the triangle diagram $\Lambda_{\mu\nu,\Delta}$ [Fig. 2(a)–2(c)], the left and right bubble diagrams $\Lambda_{\mu\nu,\mathrm{bub}_L}^\perp$ [Fig. 2(d)] and $\Lambda_{\mu\nu,\mathrm{bub}_R}^\perp$ [Fig. 2(e)], and the pole diagram $\Lambda_{\mu\nu,\mathrm{pol}_L}^\perp$ [Fig. 2(f)]. The corresponding contributions are given by

$$\Lambda^{\perp}_{\mu\nu,\mathrm{bub}_L}(p_1,p_2) = -6N_f g_{B_1^*} g_{B_2} \int dk_{123} \sum_{i=1}^{3} e_i L^{\perp}_{i\mu} \Phi(z_0) \int_0^1 dt \Phi'(z_0 + t z_i(-q)) R_{\nu,\Sigma}(k_1'^+, k_2'^+, k_3'^+), \tag{C6a}$$

$$\Lambda^{\perp}_{\mu\nu,\mathrm{bub}_R}(p_1,p_2) = -6N_f g_{B_1^*} g_{B_2} \int dk_{123} \sum_{i=1}^{3} e_i L^{\perp}_{i\mu} \Phi(z_0) \int_0^1 dt \Phi'(z_0 + t z_i(q)) R_{\nu,\Sigma}(k_1^+, k_2^+, k_3^+), \tag{C6b}$$

$$\Lambda^{\perp}_{\mu\nu,\mathrm{pol}_L}(p_1,p_2) = 6N_f g_{B_1^*} g_{B_2} \int dk_{123} \Phi^2(z_0) R_{\alpha,\Sigma}(k_1'^+, k_2'^+, k_3'^+) \tilde{S}^{\alpha\beta}_{B^*}(p_2)(g^{\perp}_{\mu\nu}\gamma_\beta - \gamma^{\perp}_{\mu} g_{\nu\beta}). \tag{C6c}$$

[1] M. Mattson *et al.* (SELEX Collaboration), Phys. Rev. Lett. **89**, 112001 (2002).
[2] V. V. Kiselev and A. K. Likhoded, Usp. Fiz. Nauk **172**, 497 (2002) [Phys. Usp. **45**, 455 (2002)].
[3] A. Faessler, T. Gutsche, M. A. Ivanov, J. G. Körner and V. E. Lyubovitskij, Phys. Rev. D **80**, 034025 (2009).
[4] M. J. White and M. J. Savage, Phys. Lett. B **271**, 410 (1991).
[5] M. A. Sanchis-Lozano, Nucl. Phys. **B440**, 251 (1995).
[6] J. M. Flynn and J. Nieves, Phys. Rev. D **76**, 017502 (2007); **77**, 099901(E) (2008).
[7] E. Hernandez, J. Nieves, and J. M. Verde-Velasco, Phys. Lett. B **663**, 234 (2008).
[8] A. Faessler, T. Gutsche, M. A. Ivanov, J. G. Körner and V. E. Lyubovitskij, Phys. Lett. B **518**, 55 (2001).
[9] C. Albertus, E. Hernandez, J. Nieves, and J. M. Verde-Velasco, Eur. Phys. J. A **32**, 183 (2007); **36**, 119(E) (2008).
[10] W. Roberts and M. Pervin, arXiv:0803.3350.
[11] C. Albertus, E. Hernandez, and J. Nieves, Phys. Lett. B **683**, 21 (2010).
[12] X. H. Guo, H. Y. Jin, and X. Q. Li, Phys. Rev. D **58**, 114007 (1998).
[13] D. Ebert, R. N. Faustov, V. O. Galkin, and A. P. Martynenko, Phys. Rev. D **70**, 014018 (2004); **77**, 079903(E) (2008).
[14] A. I. Onishchenko, arXiv:hep-ph/0006271.
[15] M. A. Ivanov, M. P. Locher, and V. E. Lyubovitskij, Few-Body Syst. **21**, 131 (1996); M. A. Ivanov, V. E. Lyubovitskij, J. G. Körner, and P. Kroll, Phys. Rev. D **56**, 348 (1997); M. A. Ivanov, J. G. Körner, V. E. Lyubovitskij, and A. G. Rusetsky, Phys. Rev. D **57**, 5632 (1998); **60**, 094002 (1999); M. A. Ivanov, J. G. Körner, V. E. Lyubovitskij, M. A. Pisarev, and A. G. Rusetsky, Phys. Rev. D **61**, 114010 (2000); A. Faessler, T. Gutsche, M. A. Ivanov, J. G. Körner, V. E. Lyubovitskij, D. Nicmorus, and K. Pumsa-ard, Phys. Rev. D **73**, 094013 (2006); A. Faessler, T. Gutsche, B. R. Holstein, V. E. Lyubovitskij, D. Nicmorus, and K. Pumsa-ard, Phys. Rev. D **74**, 074010 (2006); A. Faessler, T. Gutsche, B. R. Holstein, M. A. Ivanov, J. G. Körner, and V. E. Lyubovitskij, Phys. Rev. D **78**, 094005 (2008).
[16] W. S. Dai, X. H. Guo, H. Y. Jin, and X. Q. Li, Phys. Rev. D **62**, 114026 (2000).
[17] C. Albertus, E. Hernandez, and J. Nieves, arXiv:1004.3154.
[18] S. Weinberg, Phys. Rev. **130**, 776 (1963); A. Salam, Nuovo Cimento **25**, 224 (1962); K. Hayashi, M. Hirayama, T. Muta, N. Seto, and T. Shirafuji, Fortschr. Phys. **15**, 625 (1967).
[19] G. V. Efimov and M. A. Ivanov, *The Quark Confinement Model of Hadrons* (IOP Publishing, Bristol, 1993).
[20] S. Mandelstam, Ann. Phys. (N.Y.) **19**, 1 (1962).
[21] J. Terning, Phys. Rev. D **44**, 887 (1991).
[22] T. Branz, A. Faessler, T. Gutsche, M. A. Ivanov, J. G. Körner, and V. E. Lyubovitskij, Phys. Rev. D **81**, 034010 (2010).
[23] C. Amsler *et al.* (Particle Data Group), Phys. Lett. B **667**, 1 (2008).
[24] W. Roberts and M. Pervin, Int. J. Mod. Phys. A **23**, 2817 (2008).
[25] J. R. Zhang and M. Q. Huang, Phys. Rev. D **78**, 094015 (2008).
[26] A. Bernotas and V. Simonis, arXiv:0801.3570.
[27] J. A. M. Vermaseren, Nucl. Phys. B, Proc. Suppl. **183**, 19 (2008); arXiv:math-ph/0010025.
[28] A. Kadeer, J. G. Körner, and U. Moosbrugger, Eur. Phys. J. C **59**, 27 (2009).
[29] P. Bialas, J. G. Körner, M. Krämer, and K. Zalewski, Z. Phys. C **57**, 115 (1993).
[30] R. C. E. Devenish, T. S. Eisenschitz, and J. G. Körner, Phys. Rev. D **14**, 3063 (1976).